

THE STRUCTURAL BEHAVIOUR AND ULTIMATE STRENGTH OF REINFORCED
CONCRETE SLABS STRENGTHENED BY EPOXY-BONDED STEEL PLATES

Ibrahim Khalilullahi Zubairu

October, 1998

THE STRUCTURAL BEHAVIOUR AND ULTIMATE STRENGTH OF
REINFORCED CONCRETE SLABS STRENGTHENED BY EPOXY-BONDED
STEEL PLATES

BY

Ibrahimu Khalilullahi Zubairu

A Dissertation Submitted to the Postgraduate School, Ahmadu
Bello University, in partial fulfillment of the
requirements for the award of Doctor of Philosophy Degree
in Structural Engineering in the Department of Civil
Engineering, Faculty of Engineering, Ahmadu Bello
University, Zaria, Nigeria

October, 1998

DECLARATION

I, Ibrahim K. Zubairu hereby declare that this thesis has been prepared by me and is solely the record of my research work. That to the best of my knowledge, it has not been presented in any previous application for any degree.

All literature cited are specifically acknowledged by means of references.



Declarant

03-11-98
Date

CERTIFICATION

This thesis entitled "THE STRUCTURAL BEHAVIOUR AND ULTIMATE STRENGTH OF REINFORCED CONCRETE SLABS STRENGTHENED BY EPOXY-BONDED STEEL PLATES" by Ibrahim K. Zubairu meets the regulations governing the award of the degree of Doctor of Philosophy in Structural Engineering of Ahmadu Bello University and is approved for its contribution to knowledge and literary presentation.



Dr. S. P. Ejeh
Chairman, Supervisory Committee

98-11-04
Date



Dr. J. O. Afolayan
Member, Supervisory Committee

4-11-98
Date



Dr. K. J. Osinubi
Head, Department of Civil Engineering

4.11.98
Date



Prof. J. Y. Olayemi
Dean, Postgraduate School

20/4/99
Date

AHMADU BELLO UNIVERSITY
KASIM IBRAHIM LIBRARY

DEDICATION

This thesis is dedicated to the entire members of my family
for their endurance at the most difficult periods.

ACKNOWLEDGEMENTS

The contribution of many individuals and organisations, in whatever way to the successful completion of this study, is gratefully acknowledged. I would particularly like to express my profound gratitude to the following:

- (1) Canadian International Development Agency (CIDA), Canada for sponsoring my stay in McGill University, Montreal, Canada as a visiting scholar.
- (2) Professor Saeed M. Mirza of the Department of Civil Engineering and Applied Mechanics, McGill University, Montreal, Canada for funding the experimental work.
- (3) My employer, Ahmadu Bello University, Zaria, Nigeria for granting me study leave.
- (4) My supervisors: Dr. S. P. Ejeh and Dr. J. O. Afolayan for their guidance and invaluable suggestions throughout the study.
- (5) Several McGill University individuals and friends (like Prof. Hassan Haji Kazeem) for their hospitality and assistance in various ways during data collection and experimental work.

(6) Late Dr. A. A. Hussein for some advice and encouragement at the commencement of the study.

(7) All my working colleagues and friends in Ahmadu Bello University Zaria, Nigeria, particularly staff of Building Department for the interest and friendly atmosphere provided which was encouraging.

Above all, I thank the Almighty Allah for His divine guidance and inspiration.

ABSTRACT

The structural behaviour and ultimate strength of concrete slabs strengthened by epoxy-bonded steel plates was studied by both analytical and experimental investigations. The purpose was to evaluate their structural response at the serviceability and ultimate limit states. Simple analytical models that predict the ultimate behaviour of reinforced concrete slabs with epoxy-bonded steel plates on the tension face in the elastic and plastic regions were developed. The analytical models were evaluated by comparing analytical results with the test data for 13 slabs.

Thirteen concrete slabs were tested to failure under central point load. The measured load versus deflection at midspan of the slabs and the load versus strain in steel plate were plotted and compared with the control slabs.

The ratio of the ultimate load of plated slabs to unplated slabs was 4.78 and 1.92, for tension reinforcement ratio 0.00 and 0.71 respectively. The presence of glue alone enabled the slabs to carry higher ultimate loads by up to 45 percent. These results clearly indicated the beneficial effect of bonded plates in enhancing the ultimate flexural strength of reinforced concrete slabs.

The glued plates also reduce the deflection and steel plate strain at different rates and that the rate of reduction varies with the applied load level. However, the stiffening effect of the glued plates is much greater in controlling cracking than in controlling deflection. Comparisons of the analytical results with the test data obtained for thirteen concrete slabs were also carried out. The average ratio of experimental to theoretical ultimate moment of both plated and unplated slabs was of the order of 1.00, with a minimum of 0.64 and a maximum of 1.15. Generally, a reasonably close agreement between the calculated and measured data was noted.

The applicability of the plate bonding technique to strengthen structurally damaged reinforced concrete slabs was also examined. The structural behaviour of precracked slabs, loaded up to 45 percent of their flexural capacity, were reported. The results showed that strengthening, by epoxy-bonded steel plates, of cracked slabs is structurally efficient and that these plated slabs can carry higher ultimate load from 72 to 98 percent of the original unplated slabs. The restraining effect of the steel plates on the existing cracks was, however, more pronounced when the load was increased beyond the original preloading value.

To explore the effectiveness of the epoxy give in preserving composite action, slippage at the interface was measured. The results revealed that provided epoxy with a wide range of strengths and ductilities are used and adequate precautions are observed in the gluing technique, both slab action and full composite behaviour can be maintained until failure. Slip measurements for the set of test slabs varied from 0.018 to 1.930 mm.

TABLE OF CONTENTS

<u>Chapter</u>	<u>Page</u>
Title Page	i
Declaration	ii
Certification	iii
Dedication	iv
Acknowledgements	v
Abstract	vii
Table of Contents	x
List of Tables	xiii
List of Figures	xiv
List of Plates	xv
List of Appendices	xvi
List of Symbols	xvii
1. INTRODUCTION	1
1.1 Background	1
1.2 Need for the Research	3
1.3 Aim and Objectives of the Research	4
1.4 Scope and Limitations	4
1.5 Methodology	6
2. REVIEW OF LITERATURE	9
2.1 Preamble	9
2.2 Previous Studies	11
2.3 Applications	27
3. ANALYTICAL MODELLING OF PLATE BONDED REINFORCED CONCRETE SLABS	34
3.1 Introduction	34
3.2 Basic Assumptions	35
3.3 Calculation of Strains, Stresses and Deflection at Midspan due to Applied Load	37

<u>Chapter</u>	<u>Page</u>
3.3.1	Strains 39
3.3.2	Stresses 39
3.3.3	Forces 40
3.3.4	Location of Neutral Axis and Internal Resisting Moment ... 46
3.3.5	Applied Load 47
3.3.6	Curvature 47
3.3.7	Deflection 47
3.4	Comparison of Measured and Analytical Results 48
3.1.1	General Observations on Measured and Predicted Results ... 51
4.	EXPERIMENTAL INVESTIGATIONS 59
4.1	Materials 59
4.1.1	Concrete 59
4.1.2	Steel Reinforcement 64
4.1.3	Steel Plate 67
4.1.4	Epoxy 67
4.2	Test Specimens 70
4.2.1	Series A 73
4.2.2	Series B 73
4.2.3	Series C 74
4.2.4	Series D 75
4.3	Fabrication 75
4.4	Instrumentation 77
4.5	Test Equipment and Procedure 78
4.6	Test Results and Discussion 80
4.6.1	Deformation Properties 81
	4.6.1.1 Deflection Behaviour ... 81
	4.6.1.2 Strain Deformation ... 88
4.6.2	Composite Behaviour 93
4.6.3	Strength Properties 95
4.6.4	Cracking and Failure Characteristics 98

<u>Chapter</u>		<u>Page</u>
5.	SUMMARY, CONCLUSIONS AND RECOMMENDATIONS	... 103
5.1	Summary 103
5.2	Conclusions 105
5.3	Recommendations 108
	REFERENCES 110
	APPENDICES 116

LIST OF TABLES

<u>Table</u>	<u>Page</u>
2.1 Applications of Steel Plate Bonded for Strengthening of Concrete Structures ...	31
3.1 Geometrical and Material Properties of each Slab Series	50
3.2 Measured and Calculated Results for Slab Test Series (A) through (D)	52
3.3 Mean Values of Deflection and Ultimate Load Ratios for each Slab Series	53
3.4 Ultimate Plate Strains and Moment Capacity of Test Slabs	55
3.5 Comparison of Observed and Predicted Modes of Failure	58
4.1 Mix Design for 35 N/mm ² Concrete	60
4.2 Mechanical Properties of Concrete	63
4.3 Summary of Properties of Steel Plates and Reinforcing Bar	66
4.4 Comparison of Typical Engineering Properties of Epoxy Adhesive, Concrete and Mild Steel...	69
4.5 Typical Properties of Epoxy Adhesive used ...	70
4.6 Details of Test Slabs	72
4.7 Details of Strengthening	74
4.8 Strength and Deflection Characteristics of Test Slabs	82
4.9 Measured Ultimate Plate Strains of Test Slabs..	92
4.10 Observed Ultimate Slip of Test Slabs ...	94
4.11 Comparison of Strength Characteristics of Unplated Slab R1P0 and Plated Slabs in Series (B) and (D)	96
4.12 Comparison of Strength Characteristics of Slabs in Series (A) and (C) and Unplated Control Slab R0P0	98
4.13 Observed Modes of Failure	99

LIST OF FIGURES

<u>Figure</u>	<u>Page</u>
3.1 Slab Test Set up and Typical Cross-section ...	34
3.2 Idealized Stress-Strain Relationship for Reinforcing Bar and Steel Plates	36
3.3 Idealized Stress-Strain Curve for Concrete in Uniaxial Compression	37
3.4 Strain, Stress and Force Diagrams across Depth of Section	38
3.5 Comparison of Measured and Predicted Ultimate Moments	56
4.1 Typical Stress-Strain Curve for Concrete Cylinders Loaded in Uniaxial Compression ...	64
4.2 Uniaxial Stress-Strain Curve for Steel in Tension	66
4.3 Dimensions of a Typical Test Slab and Reinforcing Details	71
4.4 Electrical Strain Gauges Locations	78
4.5 Load - Deflection Curves for Slabs in Series A	83
4.6 Load - Deflection Curves for Slabs in Series B	84
4.7 Load - Deflection Curves for Slabs in Series C	85
4.8 Load - Deflection Curves for Slabs in Series D	88
4.9 Load versus Steel Plate Strain for Slabs in Series B	89
4.10 Load versus Steel Plate Strain for Slabs in Series C	90
4.11 Load versus Steel Plate Strain for Slabs in Series D	92

LIST OF PLATES

<u>Plate</u>	<u>Page</u>
I Concrete Cylinder Test for Compressive Strength	61
II Split - Cylinder Test for Concrete Tensile Strength	61
III Steel Uniaxial Tension Test	65
IV Reinforcement Pattern for Test Slabs ...	77
V General View of the Test Rig	80
VI Failure Patterns of the Test Slabs in Series (A) through (D)	87
VII Plate Separation and Fracture Effect ...	94
VIII Cracking Behaviour and Failure Mode for Slab Test Series (A) through (D) ...	100

LIST OF APPENDICES

<u>Appendix</u>	<u>Page</u>
I PSLAB Flowchart	116
II PSLAB Computer Program	117
III Typical Design Calculations for Test Slab ...	122

LIST OF SYMBOLS

A	=	Area under stress-strain curve of concrete
A_{pl}	=	Area of composite steel plate
A_s	=	Area of steel reinforcement
A_{si}	=	Total area of steel in level i
b	=	Width of section
b_{pl}	=	Width of steel plate
C_c	=	Concrete compressive force
D	=	Diameter of specimen
d_c	=	Depth measured from top concrete fibre to line of action of concrete compressive force
d_i	=	Distance from top concrete fibre to the centroid of steel reinforcement in layer i
d_{pl}	=	Distance from top concrete fibre to the centroid of steel plate
E_c	=	Modulus of elasticity of concrete
E_{pl}	=	Modulus of elasticity of steel plate
E_s	=	Young's modulus of steel reinforcement
F	=	Force in steel plate
f_c	=	Stress in concrete
f'_c	=	Concrete compressive strength in test cylinder
f''_c	=	Concrete maximum compressive strength
f_{pl}	=	Steel plate stress corresponding to tensile failure strain
f_r	=	Concrete tensile strength in test cylinder
f_{si}	=	Steel reinforcement stress corresponding to strain at level i
f_y	=	Yield stress of steel reinforcement
h	=	Height of section
i	=	Level of steel reinforcement
k	=	Factor for concrete strength in member
L	=	Span of slab
l	=	Length of specimen
M	=	Internal moment
$M_{ext.}$	=	External moment due to applied load


P	=	Applied load
Q	=	First moment of area about of area under concrete stress-strain curve
t	=	Thickness of steel plate
T_i	=	Force in steel reinforcement at level i
w	=	Unit weight of concrete
X	=	Neutral axis depth measured from top of concrete compression fibre
α	=	Mean stress factor
Δ	=	Mid span deflection
e_c	=	Strain in concrete
e_c	=	Strain at centroid of area under stress-strain curve
e_{cf}	=	Strain in the extreme fibre of concrete
e_0	=	Strain in concrete at maximum stress
e_{pl}	=	Tensile failure strain of steel plate
e_{si}	=	Strain in steel reinforcement at level i
e_y	=	Yield strain of steel reinforcement
γ	=	Centroid factor indicating position of compressive force in concrete
ϕ	=	Curvature at mid span of test slab
μ	=	Micron (10^{-6})
ρ	=	Steel reinforcement ratio (A_s/bd)

CHAPTER 1

INTRODUCTION1.1 Background

The maintenance, rehabilitation and upgrading of an existing concrete structure have always been a point of interest to structural and construction engineers. Upgrading here involves strengthening of the existing members to carry higher ultimate loads and/or satisfy more stringent serviceability requirements.

The structural behaviour of an existing concrete structures may be unsatisfactory due to excessive deformation, cracking or inadequate ultimate strength. The most common causes include certain minor deficiencies in design and construction of certain structural members, functional changes, corrosion of reinforcement, damage due to flood and earthquake. In such circumstances, it is advisable to either demolish and rebuild the structure or to upgrade it by strengthening it at critical locations. In the present economic climate, the second alternative is becoming more attractive and financially viable in comparison with demolition and rebuilding which often involves heavy expenditure in the form of basic material and labour cost, besides considerable time required for reconstruction.



Methods used for strengthening elements of existing structures include external post tensioning and the addition of epoxy-bonded steel plates to the tension faces of the members. Dunker et al. (1985) and Saadatmanesh et al. (1989a, 1989b, 1989c) reported that external post-tensioning by means of high-strength strands or bars has been used successfully to increase the strength of girders in existing bridges and buildings. This method, however, presents some practical difficulties in providing anchorage for post-tensioning strands, maintaining lateral stability of the girders during post-tensioning and protecting the strands against corrosion.

The addition of epoxy-bonded steel plates to the concrete surfaces (in the tension, compression and shear zones) of members has been used effectively to strengthen both bridges and buildings in South Africa, Europe and Japan (Fleming et al., 1967; Brown, 1973; Parkinson, 1978; Dussek, 1980; Lino and Otokawa, 1981; Van Gemert, 1981; Klaiber et al., 1987; Jones et al., 1988). Investigations into the performance of the members strengthened by this technique were started in the 1960s (Lerchental 1967; Kejfasz 1967). The method is primarily used to repair and strengthen reinforced concrete elements with insufficient load carrying capacity due to mechanical damage, functional changes or corrosion of reinforcing steel. The principles of this technique are relatively quick and simple. Steel

plates are epoxy-bonded to the tension zones of structural elements (such as beams), increasing both the strength and stiffness of the member. The advantages of this technique include the ability to strengthen part of a structure while still in use, small changes in structural sizes (which are generally only in the order of a few millimetres), low cost, ease of maintenance and elimination of special anchorages needed in the post-tensioning method. A shortcoming of the method is the danger of corrosion at the epoxy-steel interface. This is however eliminated by applying an epoxy primer paint adhesive.

1.2 Need for the Research

Although the technique of bonding steel plates to concrete surfaces using epoxy resins has been used widely in practice, the behaviour of structural members strengthened by epoxy-bonded steel plates is not fully understood and its modelling is far from established. The majority of reported studies on the structural behaviour of plated beams by researchers like Kejfas (1967); Irwin (1975); MacDonald (1978); Raithby (1980); Jones et al (1980); Swamy et al (1987); Swamy et al (1989); and Jones et al (1988) were experimental. The studies do not systematically evaluate the influence of the glued plates on the deformation, strength and failure mode or present specific analytical models. Very little information

seems to be available on the structural behaviour of plated slabs. The need was therefore identified to systematically study the ultimate structural behaviour of slabs strengthened by epoxy-bonded steel plates with the view to establishing a rational method of analysis that allows for better design.

1.3 Aim and Objectives of the Research

The aim of this research work is to study the structural behaviour of plate bonded concrete slabs at the various serviceability and ultimate limit states. This is pursued through the following objectives:

- (1) To develop a simple analytical models that can be implemented in a computer program for the prediction of the ultimate behaviour of reinforced concrete slabs strengthened with epoxy-bonded steel plates in the elastic and plastic regions.
- (2) To investigate experimentally and compare the test results with the theoretically predicted values in order to evaluate the correlation between the two data obtained.

1.4 Scope and Limitations

The structural behaviour and ultimate strength of plate bonded structural elements are affected by many factors such as plate thickness, plate ultimate

strength and stiffness, concrete compressive strength, steel reinforcement ratio, glue thickness, stress concentration in the adhesive layer etc. To address the effects of some of the basic design variables, this study focused attention on developing a basic understanding of the behaviour of concrete slabs strengthened with externally bonded steel plates. Analytical models based on compatibility of deformations and equilibrium of forces were developed to simulate the structural behaviour of centrally loaded square concrete slabs strengthened by epoxy-bonded steel plates. The analysis assumed singly reinforced concrete members with rectangular cross-section; in principle, similar approaches apply for other geometric configurations.

An experimental study of 13 concrete slabs was undertaken to investigate the effect of epoxy-bonded steel plates on the structural response and ultimate strength of square concrete slabs strengthened with such steel plates. The main parameters investigated were reinforcement ratio, plate thickness, presence of epoxy layer only and slip. The test slabs included two unplated, one glued and ten plated slabs. Emphasis was given to structural deformations, cracking behaviour and collapse pattern. The results of the calculated ultimate load values along with the deflections were compared with the experimental results.

In this study, only epoxy adhesive was used to attach the steel plates to the slabs and an effort was made to limit the selection of the plates and epoxies to those which are commercially available at fairly low cost. Use of bolts to increase stiffness and improve shear transfer from plates to concrete was not considered.

1.5 Methodology

The research work was divided into three major parts; a review of literature, an analytical study and an experimental programme. Available and relevant literature were extensively reviewed to articulate existing knowledge on the chosen topic. This was followed by analytical study.

Simple analytical models based on the compatibility of deformations and equilibrium of forces were developed to predict the stresses and deformations in the concrete slabs strengthened with steel plates epoxy-bonded to their tension faces. The analytical models were coded in a computer program called PSLAB to carry out the computations (see appendix I).

The third part of the work was laboratory experiments. This programme provides test data on the effect of epoxy-bonded steel plates on the structural behaviour

and ultimate strength of plated slabs. The main variables investigated were plate thickness, steel reinforcement ratio and slip at the interface between concrete and plate.

Thirteen concrete slabs were cast and tested to failure. Eleven of the slabs were provided with external reinforcement in the form of steel plates or 3mm epoxy layer. The remaining with no steel plate or epoxy adhesive were used as control slabs. The slabs, 1100 x 1100 x 100mm, were reinforced with 19 x 4mm diameter bars at an effective depth of 75mm. The plates used for external reinforcement were of mild steel. Three plate thicknesses of 2, 3 and 4mm were used. All the slabs were simply supported along the four sides and loaded at the midspan. Six concrete cylinders measuring 152 x 305mm per slab were also cast and tested when the slabs were tested. Three cylinders each were used to determine the compressive and split tensile strengths of the concrete. The concrete in the slabs was designed for a 28-day compressive strength of about 35 N/mm².

The slabs and cylinders were demoulded after 24 hours and cured for at least 28 days in an uncontrolled internal laboratory conditions. The plates were bonded to the tension face of the concrete slabs after careful surface preparation of the concrete surfaces and plates. The slabs were then white washed and extensively instrumented. The

strains in the plates were measured through electrical resistance strain gauges, (ERS), placed at several locations in the lateral and diagonal directions. Deflection in the midspan and lateral directions was measured by means of linear variable differential transformers, (LVDT), placed on top of the slabs. Slip at the interface between plate and concrete was also measured by means of LVDTs placed at two ends in the bottom face of the slabs. Cracks were marked at each load increment. Deflection, steel plate strains and slip all monitored by means of an automatic data acquisition system. Load was measured by a load cell. The same loading rate was used for all slabs.

CHAPTER 2

REVIEW OF LITERATURE2.1 Preamble

Conventional techniques for strengthening concrete structures or for crack control can be intrusive, time consuming and expensive. An alternative method is to epoxy-bond steel plates to the surfaces of concrete structures. This method, which is in limited use for about 20 years, has been found to be effective and economical in particular applications (Mays, 1988). Details of this technique and its advantages over other methods include the relative simplicity of the application, minimum changes in structural sizes, low cost and ease of maintenance. The composite system formed by epoxy-bond steel plates relies on effective bond both at the concrete/epoxy and epoxy/steel interfaces. For flexural strengthening the composite system is analysed using conventional reinforced concrete theory taking into account a second set of steel reinforcement at the appropriate effective depth while plastic theory is used to estimate the increased ultimate moment capacity. Elastic theory applied to the transformed section is appropriate for the estimation of deflections and stresses.

In most applications the structure is not propped during plating and hence the strengthened section can only provide enhanced capacity for non-permanent loads. Since original stresses under working loads normally govern the design, the analysis (according to Mays, 1988) for increased flexural capacity typically involves:

- (1) Determining concrete and reinforcement stresses in unstrengthened section due to dead load;
- (2) determining concrete, reinforcement and external plates stresses in the strengthened section due to imposed load.
- (3) Summing up the strengthened and unstrengthened stresses and checking that acceptable working values under the total design load are not exceeded;
- (4) Checking that the ultimate moment of resistance of the strengthened section is adequate to withstand the factored ultimate loads.
- (5) Assessing shear stress distribution in the adhesive layer. Most strengthening involves simple spans where it is not possible to anchor soffit plate beyond the bearings. There is an abrupt section change within a tensile zone and this gives rise to both concentrated shear and peel stresses in the adhesive layer at the plate ends. Stress concentration factors of at least three or four over, and above, the nominal horizontal shear stress determined using elastic theory can occur (Mays, 1988).

Furthermore, the cover concrete is generally weaker in shear than either the adhesive or the interfaces. To avoid brittle cracking in the cover concrete at the plate ends two design steps are essential:

- (1) Using plates with a width/thickness ratio of at least 40 to reduce horizontal shears and
- (2) Limiting the nominal elastic horizontal shear stress in the adhesive under design loads to the tensile capacity of the concrete modified by an appropriate factor of safety. Supplementary bolting may also be used at the plate ends to reduce peel failures (Oehlers 1991).

2.2 Previous Studies

Previous researches relevant to the behaviour of the composite materials and the behaviour of the interface for various bond types mainly include:

- (1) Studies on the shear transfer capacity of different interface bonds,
- (2) Studies on the composite action of structural elements,
- (3) Studies on the repair of structural elements, and
- (4) Studies on reinforced concrete beams with bonded overlays.

The previous investigations on composite elements included wood-concrete, concrete-concrete and steel concrete

composite materials. However, the work in the areas of the concrete-concrete and steel-concrete structural elements is more relevant to this study than the work in the wood-concrete. The reason being that concrete and steel are much stronger than wood.

Strengthened structural elements and using composite materials to increase strength have been problems since the times of the Greek-Roman. Contemporary applications go back as far as 1900 with the resurfacing of deteriorated concrete surfaces with concrete on the United State of America (U.S.A.) highways (Sinno and Furr, 1970). Wood-concrete composite beams were also investigated and used in the U.S.A. in bridge construction since 1920. In bonding concrete to steel, the so-called spiral connectors were first used. This method was invented in Switzerland in connection with the Alpha Method (Chung, 1981 and Viest, 1960). In 1929, Caughey and Scott recommended projecting bolt ends as shear connectors (Cook, 1967). The adoption of welded studs as a new shear connector was first done in 1954 in the U.S.A. when a research was conducted to evaluate such connectors between structural steel and reinforced concrete. Prior to that date the most commonly used connectors were the spiral or channel types.

In the past two decades epoxy-resin compounds (ACI 318-84 and ACI 503.1R-86) have been extensively used. Epoxy was

first discovered by Dr. Pierre Castan in Switzerland in 1936 and the use of epoxy (in the construction industry) as an adhesive for bonding concrete to concrete started in 1948. In 1954, the California Division of Highways, Materials and Research Department became interested in using epoxy resins as an adhesive for the cementing of raised traffic-line markers to highway surfaces. The excellent adhesion of these markers to portland-cement concrete, prompted the Department (i.e. California Division of Highways) to investigate the possible use of epoxy-resins to the maintenance and repair of concrete highways and bridges. Through various tests and applications, epoxy was found to have the following properties:

- (1) High adhesion strength to almost every material,
- (2) Very low shrinkage during cure, short curing time and great volume stability after cure,
- (3) Good tensile strength,
- (4) High compressive strength,
- (5) Natural "gap filling" qualities,
- (6) Water impermeability,
- (7) Thermosetting (it will not melt) and
- (8) Resistance to most chemicals and electrical insulation.

Other properties, very important for engineering purposes are: fatigue resistance, abrasion resistance, creep resistance and the ability to withstand thermocycling.

These properties made the epoxy-resins to be useful in the following three major ways:

- (1) Concrete surface protection: Skid resistant, protective and wearing surfaces on concrete slabs, waterproofing membranes, anti-corrosive paint for concrete surface to prevent chemical attack, etc.
- (2) Repair: Grouting cracks in concrete, joints in masonry, etc.
- (3) Adhesive: Adhesive for bonding concrete to concrete and concrete to other materials.

Birkeland and Birkeland (1966) first introduced the shear friction theory explaining the shear behaviour of steel-concrete and concrete-concrete interfaces. A shear load when applied across an interface will produce displacements at the shear plane. The displacement perpendicular to the shear plane will result in axial tensile stresses in the interface reinforcement which will produce vertical compressive stresses and a frictional force on the interface. Later, the above theory served as the basis of the ACI Building Code requirements for shear design of concrete interfaces (ACI 318-83).

Saemann and Washa (1964) studied the shear connections between precast beams and cast-in-place slabs. In their study, 42 beams and various control cylinders were tested. They provided data on the relationships between

- (1) Concrete compressive strength versus shear stress and slip,
- (2) Shear stress versus deflection,
- (3) Shear stress versus percentage steel across the joint and
- (4) The effect of roughness on the shear stress versus deflection and on the shear stress versus slip. Data on the development of slip across the length of the beam was also provided. The tests indicated that there are complex relationships between the degree of roughness of the interface, the length of the shear span and the percentage of steel across the joint.

Sinno and Furr (1970) performed direct shear tests on thin bonded concrete overlays to evaluate the parameters involved in bonding freshly laid concrete to repair deteriorated concrete surfaces. The performance of the repaired surfaces was evaluated under static and repeated loading. During the cyclic loading, it was observed that when the overlay was in compression there was no failure but, when it was in tension, the overlay cracked vertically in the first few loading cycles while the cracks did not extend horizontally in the interface. It was found that the shear capacity of the epoxy bond was in all cases high enough to withstand the shear developed in concrete bridge decks. However, direct shear tests showed that improper surface preparation could contribute to field delamination

of the deck. Also, the thin bonded concrete overlays increased the flexural rigidity and the load capacity of the beams to much higher levels than the decrease caused by their additional dead weight.

Nawy (1984) in his studies evaluated the shear transfer of two layered concrete beams. Using different amount of shear reinforcement, he investigated the relationship between bond shear capacity and strength of composite member. He provided empirical expressions for the shear capacity of the composite elements corresponding to different amount of shear reinforcement at the interface.

Moss (1984) reported on the usage and performance of epoxy resins in civil engineering, with particular regard to reinforced concrete work. The report described:

- (1) The nature of epoxy resins and some factors that affect their performance and use,
- (2) Experimental work on epoxy resin interface for steel-concrete and concrete-concrete composite beams and
- (3) Suggestions made for the specification of epoxy resins.

It also shows the behaviour of epoxy resins in structural connections, as mortars for concrete repairs and as fluids for floor coverings and coatings. The performance and effectiveness of epoxies can vary enormously between

success and total failure. The report attempted to override the scepticism on the use of epoxy resins by many engineers in helping the understanding on the proper use of the epoxy products.

Mays and Hutchinson (1988) also described the engineering property requirements for structural adhesives. They highlighted the important considerations for joint durability and proposed compliance spectrum for a two-part cold cure adhesive for the structural bonding of steel to concrete.

Plechnik et al (1986) investigated the strength properties of epoxy repaired concrete beams during and after fire exposure and future earthquakes. They found that both short-term strength and stiffness of such beams reduced rapidly at uniform temperatures exceeding about 250°F (121°C). Under fire conditions, the strength reduction was primarily influenced by the presence or lack of fire protection coatings and thermal gradient. Analytical techniques were also presented for strength analysis of epoxy repaired beams under elevated temperature or fire.

Chung (1975, 1977, 1978 and 1981) studied the repair of structural elements using epoxy-resin techniques. He found that the flexural strength of the epoxy-repaired reinforced

concrete beams was not less than the original strength and that in joint tests, the shear capacity and deformation were similar for both the repaired and the control specimen. Proper injection of epoxy during the repair tests revealed that restoration of the bond strength associated with a smaller bond slip could be achieved. In addition, in pull out tests he found that the repaired concrete joint better withstood the shear stress while the adjacent concrete failed especially when applying cyclic load and that the epoxy was stronger than the concrete itself.

Fleming and King (1967) strengthened concrete beams with the use of thin steel plates glued in the tension side. The beams failed from crushing of concrete without interface failure and yield of the steel.

Irwin (1975) found in testing beams with epoxy bonded steel plates that such beams had a 20 percent higher ultimate load capacity than beams without the epoxy connection.

Jones et al. (1980) reported the test results of eighteen reinforced concrete beams strengthened with steel plates bonded by epoxy glued to the tension face of the beams. Two series of beams were tested. Series A beams had square cross-sections of 150 x 150mm and spans 710mm. Series B beams had rectangular cross-section of 100 x 150mm and spans 1200mm. Two types of glue and two types of steel

plates with different yield strengths were used, and the effects of glue thickness, plate lapping, multiple plates and precracking prior to bonding were investigated. The effect of these variables on structural behaviour of the tested beams were discussed, and drew the following conclusions:

- (1) Epoxy-bonded steel plate enlarged the range of elastic behaviour,
- (2) Reduction in the tension stresses in the concrete,
- (3) Delayed appearance of first visual cracks with a resulting increase in the service loads,
- (4) Increased flexural strength and stiffness and
- (5) Increased the ductility at flexural failure. They also concluded that a glue thickness of about 1.0 to 1.5mm was the most appropriate for this type of application.

MacDonald and Calder (1982) studied the behaviour of concrete beams externally reinforced with steel plates bonded to their tension flanges. They tested a series of 3.5 m long and 4.9m long beams in four points load. Each beam had a rectangular cross-section of 150 x 250mm. Results obtained showed that full composite action was provided by the adhesive and that substantial improvements in performance could be achieved in terms of ultimate load, crack control and stiffness. Exposure tests were carried out on 0.5m plain concrete beams with steel plates bonded to one face. It was found that the steel may corrode

significantly during natural exposure, causing a loss in bond strength at the steel-epoxy interface. The reduction in the overall strength of the exposed beams was attributed to the corrosion.

VanGemert and VandenBosch (1985) reported the results of durability tests on concrete beams with epoxy-bonded external steel reinforcements. They studied the effects of long-term exposure, fatigue and temperature loading, concluding that the effects of atmospheric corrosion depended for the greater part on the preparation of concrete and steel plate surfaces and on the workmanship of the repair crew. Therefore, more specialised personnel and careful control of the preparation work will be necessary. Cyclic loading tests were performed on two beams with spans of 6m each. The beams were reinforced with a double layer of glued steel plates. The cross-section of the beams was 300 x 250mm; the steel plates were 5mm thick by 200mm wide.

The beams were tested under four-point bending, and they were subjected to cyclic loads resulting in a maximum stress of 40 N/mm². The loading frequency was 30 cycles/minute, and 500,000 cycles of loads were applied to each beam. The fatigue tests showed that no redistribution of stresses took place by deformation in the glue or by any failure of the glue connection. Full-scale temperature loading tests in the temperature range from -20°C to +90°C

were also conducted on specimens glued with EPICOL U epoxy adhesive. It was found that the cold-hardening epoxy glue had a poor thermal resistance and there was no decrease of the ultimate load for lower temperatures. At higher temperatures, however, the situation was different. At a temperature of about 60°C, the glue started to become weaker and more deformable. At lower temperatures, the crack always started at the end of the plate and moved into the concrete. At higher temperatures, the epoxy joint was not able to transfer the shearing stresses from the steel plate to the concrete, and a crack propagated through the epoxy joint, starting at the plate end. The performance of the epoxy joint was strongly reduced at higher temperatures.

Swamy et al. (1987) investigated the effect of glued plates on the serviceability and ultimate load behaviour of reinforced concrete beams. Twenty-four beams were tested. Each beam was 2.5m long and had a rectangular cross-section of 155 x 255mm. The beams were reinforced with three 20mm diameter bars at an effective depth of 220mm. Three glue thicknesses of 1.5mm, 3mm and 6mm were used and for each glue thickness, three plate thicknesses were used: 1.5mm, 3mm and 6mm, all of constant width of 125mm. For comparison, several beams were tested with lap plates, double plates and variable thickness for the glue along the length of the beam. The adhesive thickness varied from 3mm to 8mm. The results obtained indicated that the addition of

glued steel plates to a reinforced concrete beam could substantially increase the flexural stiffness, reduce cracking and structural deformations at all load levels, and contribute to the ultimate flexural capacity. The net effect of reduced structural deformations was that the serviceability loads were substantially increased by the stiffening action of the glued plates. It was further observed that lapped plates, precracking prior to plating, variable glue thickness and the presence of stress concentrations in the adhesive all had no adverse effect on the structural behaviour of the plated beams.

Ladner (1983) derived a set of lower and upper limits for the total reinforcement ratio (internal and external) to ensure that it would yield before the concrete failure in the compression zone. He also showed that the flexural capacity of externally reinforced concrete beams could be determined from existing ultimate strength methods of analysis by simply considering the plates to act as part of the reinforcement. The results of these analyses had shown that the plate was much more effective than reinforcing bars because of its greater lever arm. However, as the plate was not enclosed and hence not "gripped" by the concrete, as in the case of the reinforcing bars, much research has gone into studying the premature failure due to separation between the plate and the concrete, which was referred to as peeling.

Johnson and Tait (1981) tested specimens in which the plates terminated in regions of shear, flexure and axial loads; VanGemert (1981) in regions of pure shears; Ong and Cusens (1982) in regions of bearing stress; Jones et al. (1988) in the regions of shear and flexure and Oehlers (1988) studied the problem of flexural peeling stresses on the serviceability and ultimate strength of upgraded concrete beams. It appeared from these studies that two distinct forms of failure can occur:

- (1) shear peeling, induced by the formation of shear diagonal cracks and which is associated with rapid separation of the plate; and
- (2) flexural peeling, induced by increasing curvature and associated with a gradual separation of the plate. Equations were developed to predict the ultimate peeling moment that caused the complete separation of the plate from the beam, and serviceability peeling moments that caused the initial formation of peeling cracks. It was concluded that the peeling strength depended on the flexural rigidity of the cracked plated section, and it did not depend on the previous loading history of the beam or the initial curvature of the beam. The research also provided few design rules for preventing peeling such as restricting the width and the thickness of the beam and the neutral axis depth of the beam. More recent theoretical research by Robert and Haji-Kazemi (1989) and

experimental tests by Oehlers and Moran (1990) indicated that peeling can be induced by shear as well as flexural forces.

Oehlers and Moran (1990,1992) showed that externally bonded plates had a tendency to peel away after the formation of shear diagonal cracks (before the design load was reached) or when the curvature of the beam was increased. Fifty seven plated reinforced concrete beams were tested to study peeling induced by increasing curvature. In these tests, the geometry and material properties of the beams were varied, and the beams were subjected to pre-cracking and pre-cambering, as might occur in an existing structure. The results were used to formulate a design method to prevent debonding due to peeling for beams strengthened by gluing mild steel plates to their tension faces. This method determined the moment at which peeling started (serviceability limit) and the moment that caused complete separation of the plate (ultimate limit). The peeling strength due to flexural forces was found to be dependent on the flexural rigidity of the cracked plated section, the tensile strength of the concrete and the thickness of the plate. The strength was however, independent of the previous loading history of the beam, or the initial curvature of the beam and the method of clamping the plate to the beam on gluing. Beams plated over part of their width were found to have an increased flexural peeling

strength. Furthermore, it was found that debonding at the plate ends due to shear forces was not influenced by the presence of stirrups and depended on the formation of the diagonal shear crack as measured by the shear strength of the unplated structure without stirrups, so that limiting the shear flow at the steel-plate-concrete-slab interface would not prevent this form of debonding. It has also been found that this system is better suited for the strengthening of reinforced concrete slabs than reinforced concrete beams, although it enhances the serviceability requirements of both types of structures.

Hamoush and Ahmad (1990) investigated the behaviour of damaged concrete beams strengthened by externally bonded steel plates, using linear-elastic fracture mechanics and finite element method. The study investigated the failure by interface debonding of the steel plate and later the adhesive as a result of interfacial shear stresses. Simply supported concrete beams under monotonically increasing symmetrical loads were considered. The following parameters were studied: the effect of vertical flexural cracks in the concrete and the interfacial crack between the steel plate and epoxy layer upon the ultimate load capacity, and the thickness of epoxy layer and the position of external load upon the changes in the strain energy release rate and the stress intensity factors. The study also assumed that the horizontal interface cracks between the steel plate and

adhesive layer were developed from the bottom tip of the flexural crack nearest to the support, and extended horizontally outward toward the supports. The following conclusions were drawn:

- (1) For undamaged concrete beams, the strain energy release rate for an interface crack between steel plate and adhesive layer was negligibly small, and the steel plate-strengthened beam has high interface debonding load;
- (2) The strain energy release rate initially reached a maximum value when the length of the interface crack was approximately equal to the length of the flexural cracks;
- (3) The existence of a large number of flexural cracks (more than five) released the shear stress at the interface, and that led to a reduction in the strain energy release rate and stress intensity factors;
- (4) For the range of thickness of the adhesive studied ($2.5 \leq t \leq 6.35\text{mm}$), no noticeable effect on the strain energy release rate and the stress intensity factors was observed.

Saadatmanesh and Ehsani (1991) reported preliminary results from the study of reinforced concrete beams with glass fibre-reinforced plastic (GFRP) sheets bonded on the tension zone. Their work emphasized that the selection of the appropriate adhesive was of primary importance in the mechanical performance of the strengthened members.

Triantafillou and Plevris (1992) used the strain compatibility method, concept of fracture mechanics and a simple model for the fibre reinforced plastic (FRP) peeling-off mechanism to provide a systematic approach to the study of the short-term flexural behaviour of reinforced concrete beams strengthened with externally bonded composite sheets. Results of four-point bending tests were used to confirm their analysis.

Other reports by Solomon and Gopalani (1979), Raithby (1980), Lloyd et al.(1982), Raju and Nadgir (1991), Rao et al (1992) and Kar and Sharma (1992) are also available. The reports discussed various aspects of the behaviour of concrete beams externally reinforced with epoxy-bonded steel plates and in each case the effectiveness of this strengthening technique for strengthening concrete flexural members in existing structures was attested.

2.3 Applications

The technique of strengthening reinforced concrete members in situ by externally epoxy-bonded steel plates has been widely used in various parts of the world - for buildings as well as for bridges. The first recorded case was in Durban, South Africa, in 1964, where epoxy-bonded steel plates were used to strengthen concrete beams in an apartment complex (Dusseck, 1980), where part of the reinforcing steel in

the building had been accidentally omitted during construction.

In the former USSR in 1974, a 60-year old continuous-span reinforced concrete bridge was repaired with bonded plates (Klaiber, et al. 1987). Twenty-five percent of the reinforcement in the original bridge had corroded away because of poor drainage. In the negative moment region, steel plates were bonded to the clean deck surface. In the positive moment region, bolts were welded to the exposed reinforcing steel and plates were bolted and bonded to the underside of the beam. The bridge remained open to the traffic while being repaired.

Four bridges on the M5 Motorway at Quinton Interchange, Worcestershire and two bridges on the M25 - M20 Motorway Interchange at Swanley, Kent, in England were strengthened by plating in 1975 and 1977, respectively (Dusseck, 1980). At Quinton, cracks were discovered in the soffits of the end and main spans during a routine inspection of the bridges. These bridges were constructed of box-reinforced concrete slabs and they were continuous over three spans of 16.75m, 27.40m and 16.75m. Calculations indicated that inadequate tension reinforcement had been originally provided in parts of the end spans and in the edge of the main spans. Two alternative repair methods were considered: (1) Prestressing with cables; and (2) bonding steel plates.

Several bridges on an elevated highway in Japan have been strengthened with epoxy-bonded steel plates (Maeda et al., 1980). Many of the slabs in these bridges had cracked, displayed excessive spalling and scaling, or had insufficient reinforcement. Thin steel plates were bonded to the bottom of the slabs with epoxy adhesive and anchor bolts. Two construction methods were used: in one case, the adhesive was applied to the steel and concrete surfaces prior to setting; in the other, the plate was set in place first and then a liquid resin was injected in the space between the concrete slab and steel plate.

More recently, the precast, prestressed hollow-box beam skew bridge at Rotherham was limited to a maximum vehicle loading of 100 tonnes. Strengthening of this bridge to carry an abnormal load of 465 tonnes was effected by steel plates bonded transversely to the soffit of the deck. Another heavily skewed reinforced concrete bridge in Deryshire was also strengthened by externally bonded steel plate reinforcement (Swamy et al., 1989). There are many other applications of epoxy-bonded steel plates to concrete girders. In each case, the girder strength was significantly increased by bonding steel plates to the tension flange. The practical applications of this strengthening method are shown in table 2.1.

Table 2.1 Applications of Steel Plate Bonded for Strengthening of Concrete Structures

Date	Structure/Location	Reason for Strengthening	Remark	Reference
1964	Concrete beams in an apartment complex in Durban, South Africa	Accidental omission of part of reinforcement during construction	Low reinforcement ratio	Dussek, 1980
1974	60-year old continuous span reinforced concrete bridge in the former USSR	25% of the reinforcement in the original bridge corroded away due to poor drainage	Steel plates were bonded to the negative and positive moment regions	Klaiber, et al. 1987
1975	Quinton bridges M5 motorway near Birmingham, UK	Design checks indicated that bridges would not meet flexural service-ability requirements for heavy vehicles	Load tests indicated that flexural stiffness had increased by 11% and crack opening under load reduced by 35-40%.	Dussek, 1980

Table 2.1 Cont.

Date	Structure/Location	Reason for Strengthening	Remark	Reference
1977	Swanley bridges M20/M25 motorways, Kent, England	Development of flexural cracks suggesting inadequate longitudinal reinforcement of deck slabs	Scheme initiated, remedial work performed and loading tests completed in four months	Dusseck, 1980
1978	Several buildings in Zurich, Switzerland	Increased floor loadings following change in use	Flexural strength was upgraded by plating and existing structure provided a factor of safety of at least 1.1 in the event of fire	Arandit, 1979
1979	Several bridges in an elevated highway in Japan	Many slabs in these bridges had cracked, displayed excessive spalling and scaling or had insufficient reinforcement	Steel plates were bonded to the bottom of the slabs with epoxy resin and anchor bolts	Maeda, et al. 1980

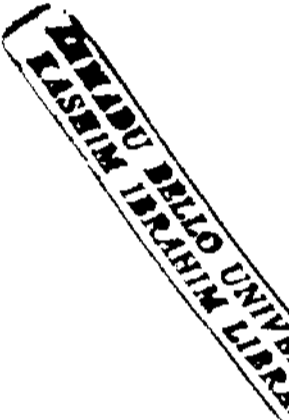


Table 2.1 Cont.

Date	Structure/Location	Reason for Strengthening	Remark	Reference
1979	Several reinforced and prestressed concrete bridges in Poland	Calculations indicated that inadequate reinforcement had been originally provided in parts of the end spans and in the edges of the main spans	Flat steel strips bonded to the upper surface of the slab in negative moment areas. Also steel plates were bonded to the underside of concrete bridge decks	Klaiber, et al. 1987
1982	Brinsworth road bridge, MI motorway near Rotherham, UK	Additional lateral reinforcement required to allow a 467 tonne load to be transported up the motorway	Deflections were considerably less than those predicted as vehicles crossed bridge; strengthening completed in five months	Swamy, et al. 1989
1982	Skewed reinforced concrete bridge in Derbyshire, UK	Additional transverse reinforcement required to carry an increased load	Load tests revealed the significant increase in strength	Swamy, et al. 1989

ANALYTICAL MODELLING OF PLATE BONDED
REINFORCED CONCRETE SLABS

3.1 Introduction

The stresses in the steel plates, concrete slabs and the deflection at midspan of simply supported concrete slabs strengthened with epoxy-bonded steel plates, subjected to centrally applied concentrated load were calculated. An incremental deformation technique based on the principles of equilibrium of forces and compatibility of deformations was used to determine the state of the stresses and deformations in the slabs. A typical cross-section used in the analytical study is shown in Fig. 3.1. The steel plate has width b_{pl} , thickness t , Young's modulus E_{pl} and tensile failure strain ϵ_{pl} , the concrete has compressive strength f'_c , strain ϵ_c and Young's modulus E_c ; and the steel reinforcement has area A_s , Young's modulus E_s and yield stress f_y . The method presented herein for the numerical solution is general and is applicable to different types of loading and support conditions.

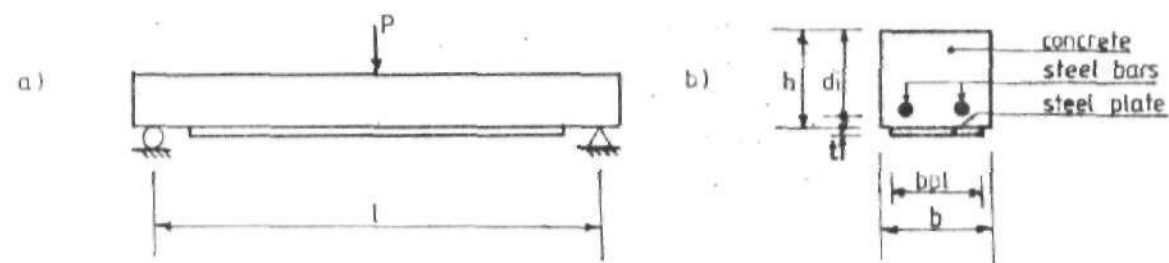


Fig. 3.1 Slab Test Set up and Typical Cross-section

3.2 Basic Assumptions

The basic assumptions made in the analysis were the following:

- (1) Slabs were assumed to be simply supported and loaded with a concentrated load at the centre (Fig. 3.1 above). This assumption was necessary in order to compare the results with the available measured data. The model can be easily modified to analyse slabs with other load distributions.
- (2) As the slab is bent, plane sections within the slab and plate were assumed to remain plane (Bernoulli's theorem). This also means that the distribution of strain across the slab and across plate is linear. However, due to possible slippage at the interface, the strain at the interface may be discontinuous.
- (3) The stress-strain relationship for the reinforcing bars and steel plate were assumed to be elastic-perfectly plastic with strain hardening effect included (Fig. 3.2). This effect can be neglected if ACI 318-83 (ACI 1983) idealization was selected. The strain hardening effect was included because test data have indicated an increase in the load capacity due to strain hardening.

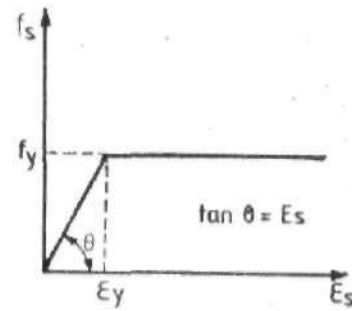


Fig. 3.2 Idealised Stress-Strain Relationship for Reinforcing Bar and Steel Plates

- (4) Full interaction at the interface bond between the plate and the slab was assumed.
- (5) Perfect bond was assumed at the interface as well as between the steel reinforcement and the concrete.
- (6) The curvatures of the slabs and the composite plate during bending are the same and therefore, no debonding was allowed slab.
- (7) Hognestad's parabola of idealized stress-strain curves for concrete in uniaxial compression was assumed. Fig. 3.3 shows the stress-strain curve of concrete, where $f''_c = kf'_c$ = the maximum compressive stress reached in the concrete of a flexural member; k = stress block parameter at flexural strength of rectangular section (Park and Paulay 1975); f'_c = concrete compressive strength; f_c = stress in concrete; ϵ_0 = strain in concrete at maximum stress; ϵ_c = strain in concrete and E_c = initial tangent modulus of concrete. The ultimate concrete strain was assumed equal to 0.0035 (mm/mm) while the concrete tensile strength was neglected.

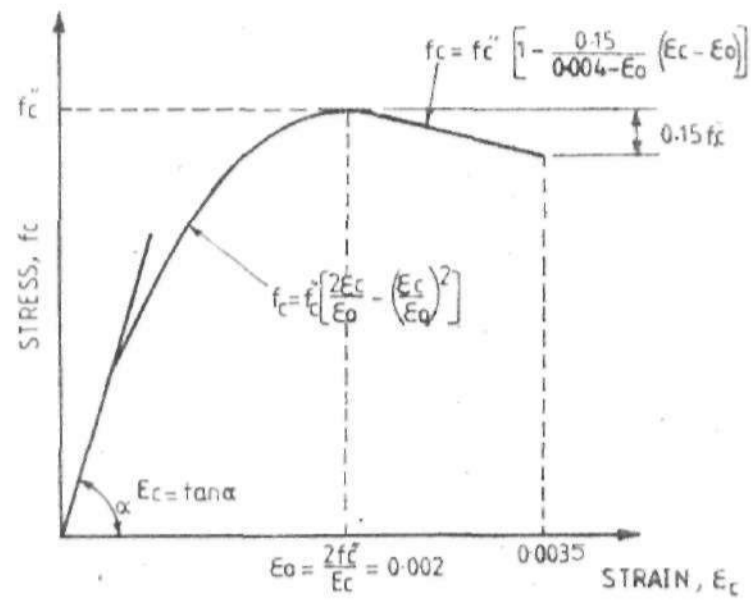


Fig. 3.3 Idealised Stress-Strain Curve for Concrete in Uniaxial Compression

- (8) The composite slab fails when either the concrete strain reaches 0.0035 or the composite steel plate reaches its ultimate strain. Because the composite slab was assumed to have sufficient shear strength, no shear deformation considerations were made in the analysis.
- (9) Small deflections.
- (10) Temperature and shrinkage stresses were ignored.

3.3 Calculation of Strains, Stresses and Deflection at Midspan due to Applied Load

The strains and stresses across the depth of the section and the curvature at midspan, were calculated based on the assumptions above. Fig. 3.4 shows the strains and stresses across the depth of the section with a composite steel plate bonded to the tension face.

For ease of calculations instead of incrementing the load, the strain in the extreme fibre of concrete, ϵ_{cf} , was increased in specified increments to generate the load-deflection curves. After each increment of strain the location of the neutral axis was iteratively calculated until the equilibrium of forces across the depth of the section is achieved. The internal resisting moment was calculated by summing the moments of all the internal forces about the neutral axis. The corresponding applied load was then found by equating the internal resisting moment and the moment produced by the applied load.

The strains, stresses and the forces across the depth of the cross section were calculated as follows:

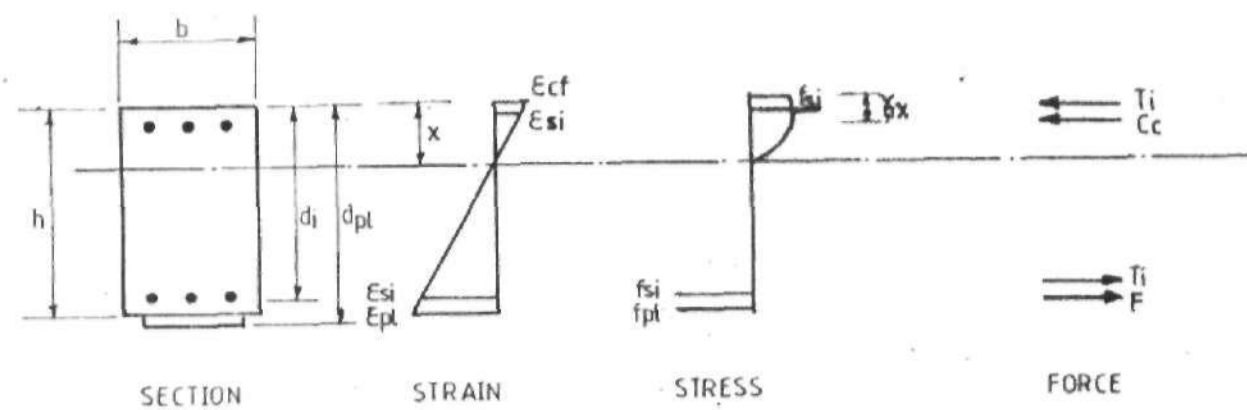


Fig. 3.4 Strain, Stress and Force Diagrams across Depth of Section

3.3.1 Strains:

The strain diagram is shown in Fig. 3.4 above. The strain in the extreme fibre of concrete in compression at midspan ϵ_{cf} was increased until failure is reached. It is assumed that failure is reached when either the concrete strain reaches 0.0035 or the composite steel plate reaches its ultimate strain. The strains in the reinforcing bars and composite steel plates were calculated in terms of ϵ_{cf} (strain in the extreme fibre of concrete) and an unknown location of neutral axis, X , using similar triangles in the strain diagram from the following equations:

$$\epsilon_{si} = \epsilon_{cf} \frac{x - d_i}{x} \quad (3.1)$$

$$\epsilon_{pi} = \epsilon_{cf} \frac{x - d_{pi}}{x} \quad (3.2)$$

where ϵ_{cf} = assumed and then increased in specified increments; ϵ_{si} = strain in steel reinforcement at level i ; X = distance to neutral axis measured from top concrete fibre; d_i = distance from top concrete fibre to centroid of steel reinforcement in layer i ; ϵ_{pi} = strain in composite steel plate and d_{pi} = distance from top concrete fibre to centroid of composite plate.

3.3.2 Stresses:

The steel reinforcement stresses f_{si} and steel plate stress f_{pi} corresponding to strains ϵ_{si} and ϵ_{pi} were found from the stress-strain curves for steel reinforcement and steel

plate (Fig. 3.4 above)

$$f_s = E_s \epsilon_s \quad \text{if } \epsilon_s \leq \epsilon_y \quad (3.3)$$

$$f_s = f_y \quad \text{if } \epsilon_s > \epsilon_y \quad (3.4)$$

$$f_p = E_p \epsilon_p \quad (3.5)$$

where E_s = modulus of elasticity of steel reinforcement; ϵ_y = yield strain of steel reinforcement and E_p = modulus of elasticity of composite plate.

3.3.3 Forces:

The steel reinforcement forces T_i and plate force, F were found by multiplying the steel stresses by their corresponding areas and the plate stress by plate area, respectively

$$T_i = f_s A_{si} \quad (3.6)$$

$$F = f_p A_p \quad (3.7)$$

where A_{si} = total area of steel in layer i ; and A_p = area of composite steel plate.

The distribution of concrete stresses in compression zone was found from the Hognestard's stress-strain curve of concrete (Fig. 3.3). The concrete stresses in the elastic and elastic-plastic regions (based on Hognestard et al. 1955) were expressed as follows:

$$f_c = f_c' \left[\frac{2\epsilon_c}{\epsilon_o} - \left(\frac{\epsilon_c}{\epsilon_o} \right)^2 \right] \quad \text{if } 0 \leq \epsilon_c < \epsilon_o \quad (3.8)$$

and

$$f_c = f_c' \left[1 - \frac{0.15}{0.004 - \epsilon_o} (\epsilon_c - \epsilon_o) \right] \quad \text{if } \epsilon_o \leq \epsilon_c \leq 0.0035 \quad (3.9)$$

For any given concrete strain in the extreme compression fibre ϵ_{cf} , the concrete compression force C_c is expressed in terms of a parameter α , defined as follows (Park and Paulay 1975).

$$C_c = \alpha f_c' b x \quad (3.10)$$

The parameter α (mean stress factor) was used to convert the nonlinear, stress-strain relationship into an equivalent rectangular stress-strain curve. It was calculated by equating the area under the stress-strain curve to an equivalent rectangular area

$$A = \int_0^{\epsilon_d} f_c \delta \epsilon_c = \alpha f_c' \epsilon_d \quad (3.11)$$

where A = area under stress-strain curve of concrete (see Fig. 3.3). Then, α was obtained from

$$\alpha = \frac{\int_0^{\epsilon_d} f_c \delta \epsilon_c}{f_c' \epsilon_d} \quad (3.12)$$

The right side of equation (3.12) was evaluated for the values of d as follows:

(i) If $0 \leq e_{cf} < e_0$, and substituting the value of f_c from equation (3.8), then

$$\alpha = \frac{\int_0^{e_{cf}} f_c'' \left[\frac{2e_c}{e_0} - \left(\frac{e_c}{e_0} \right)^2 \right] \delta e_c}{f_c'' e_{cf}}$$

$$= \frac{1}{e_{cf}} \left[\frac{e_c^2}{e_0} - \frac{e_c^3}{3e_0^2} \right]_0^{e_{cf}} = \frac{1}{e_{cf}} \left[\frac{e_{cf}^2}{e_0} - \frac{e_{cf}^3}{3e_0^2} \right] = 0$$

Therefore,

$$\alpha = \frac{e_{cf}}{e_0} - \frac{e_{cf}^2}{3e_0^2} \quad (3.13)$$

(ii) If $e_0 \leq e_{cf} \leq 0.0035$, and substituting the values of f_c from equations (3.8) and (3.9), then

$$\alpha = \frac{\int_0^{e_0} f_c \delta e_c}{f_c'' e_{cf}} + \frac{\int_{e_0}^{e_{cf}} f_c \delta e_c}{f_c'' e_{cf}}$$

$$= \frac{e_{cf}}{e_0} - \frac{e_{cf}^2}{3e_0^2} + \frac{\int_{e_0}^{e_{cf}} f_c'' \left[1 - \frac{0.15}{0.004 - e_0} (e_c - e_0) \right] \delta e_c}{f_c'' e_{cf}}$$

$$= \frac{e_{cf}}{e_0} - \frac{e_{cf}^2}{3e_0^2} + \frac{1}{e_{cf}} \left[e_0 - \frac{0.15}{0.004 - e_0} \frac{(e_c - e_0)^2}{2} \right]_{e_0}^{e_{cf}}$$

$$= \frac{e_{cf}}{e_0} - \frac{e_{cf}^2}{3e_0^2} + \frac{1}{e_{cf}} \left[e_{cf} - \frac{0.15}{0.004 - e_0} \frac{(e_{cf} - e_0)^2}{2} \right] - \frac{e_0}{e_{cf}}$$

$$= \frac{e_{cf}}{e_0} - \frac{e_{cf}^2}{3e_0^2} + 1 - \frac{0.15}{0.004 - e_0} \left(\frac{e_{cf}}{2} - e_0 + \frac{e_0^2}{2e_{cf}} \right) - \frac{e_0}{e_{cf}}$$

Therefore,

$$\alpha = 1 + \frac{\epsilon_{cf}}{\epsilon_o} \left(1 - \frac{\epsilon_{cf}}{3\epsilon_o} - \frac{\epsilon_o^2}{\epsilon_{cf}^2} \right) - \frac{0.15}{0.004 - \epsilon_o} \left(\frac{\epsilon_{cf}}{2} - \epsilon_o \right) - \frac{0.075}{0.004 - \epsilon_o} \left(\frac{\epsilon_o^2}{\epsilon_{cf}} \right) \quad (3.14)$$

The position of concrete compressive force C_c , measured from the top fibre of concrete, was expressed in terms of the parameter γ , shown in Fig. 3.4 and calculated as follows

$$d_c = \gamma x \quad (3.15)$$

where d_c = distance from top concrete fibre to line of action of concrete compressive force.

The first moment of area under the concrete stress-strain diagram about the origin Q is given by

$$Q = \int_0^{\epsilon_{cf}} f_c \epsilon_c \delta \epsilon_c = \bar{\epsilon}_c A \quad (3.16)$$

where ϵ_c = strain at centroid of area under stress-strain diagram.

The strain at centroid ϵ_c can be defined in terms of ϵ_{cf} by

$$\bar{\epsilon}_c = (1 - \gamma) \epsilon_{cf} \quad (3.17)$$

and therefore

$$Q = \bar{\epsilon}_c A = (1 - \gamma) \epsilon_{cf} \int_0^{\epsilon_{cf}} f_c \delta \epsilon_c \quad (3.18)$$

The parameter γ (centroid factor) was obtained by equating (3.16) and (3.18)

$$\gamma = 1 - \frac{\int_0^{\epsilon_{cf}} \epsilon_c f_c \delta \epsilon_c}{\epsilon_{cf} \int_0^{\epsilon_{cf}} f_c \delta \epsilon_c} \quad (3.19)$$

Equation (3.19) was evaluated for values of γ in the concrete slab both in the elastic and elastic-plastic regions by integrating the concrete stresses over the slab area as follows:

(i) If $0 \leq \epsilon_{cf} < \epsilon_0$, and substituting the value of f_c from equation (3.8), then

$$\begin{aligned} \gamma &= 1 - \frac{\int_0^{\epsilon_{cf}} \epsilon_c f_c'' \left[\frac{2\epsilon_c}{\epsilon_0} - \left(\frac{\epsilon_c}{\epsilon_0} \right)^2 \right] \delta \epsilon_c}{\epsilon_{cf} \int_0^{\epsilon_{cf}} f_c'' \left[\frac{2\epsilon_c}{\epsilon_0} - \left(\frac{\epsilon_c}{\epsilon_0} \right)^2 \right] \delta \epsilon_c} \\ &= 1 - \frac{\left[\frac{2\epsilon_c^3}{3\epsilon_0} - \frac{\epsilon_c^4}{4\epsilon_0^2} \right]_0^{\epsilon_{cf}}}{\epsilon_{cf} \left[\frac{\epsilon_c^2}{\epsilon_0} - \frac{\epsilon_c^3}{3\epsilon_0^2} \right]_0^{\epsilon_{cf}}} = 1 - \frac{\left[\frac{2\epsilon_{cf}^3}{3\epsilon_0} - \frac{\epsilon_{cf}^4}{4\epsilon_0^2} \right] - 0}{\epsilon_{cf} \left[\frac{\epsilon_{cf}^2}{\epsilon_0} - \frac{\epsilon_{cf}^3}{3\epsilon_0^2} \right] - 0} \\ &= 1 - \frac{\frac{1}{\epsilon_0} \left(\frac{2}{3} - \frac{\epsilon_{cf}}{4\epsilon_0} \right)}{\frac{1}{\epsilon_0} \left(1 - \frac{\epsilon_{cf}}{3\epsilon_0} \right)} = 1 - \frac{\left(\frac{8\epsilon_0 - 3\epsilon_{cf}}{12\epsilon_0} \right)}{\left(\frac{3\epsilon_0 - \epsilon_{cf}}{3\epsilon_0} \right)} = \frac{4\epsilon_0 - \epsilon_{cf}}{12\epsilon_0 - 4\epsilon_{cf}} \end{aligned}$$

Dividing right hand side through by $12\epsilon_0$

$$\gamma = \frac{\frac{1}{3} - \frac{\epsilon_{cf}}{12\epsilon_0}}{1 - \frac{\epsilon_{cf}}{3\epsilon_0}} \quad (3.20)$$

(ii) If $\epsilon_0 \leq \epsilon_{cf} \leq 0.0035$, and substituting the values of f_c from equations (3.8) and (3.9), then

$$\begin{aligned} \gamma &= 1 - \frac{\int_0^{\epsilon_0} \epsilon_c f_c \delta \epsilon_c + \int_{\epsilon_0}^{\epsilon_{cf}} \epsilon_c f_c \delta \epsilon_c}{\epsilon_{cf} \int_0^{\epsilon_{cf}} f_c \delta \epsilon_c + \epsilon_{cf} \int_{\epsilon_0}^{\epsilon_{cf}} f_c \delta \epsilon_c} \\ &= 1 - \frac{\int_0^{\epsilon_0} \epsilon_c f_c'' \left[\frac{2\epsilon_c}{\epsilon_0} - \left(\frac{\epsilon_c}{\epsilon_0} \right)^2 \right] \delta \epsilon_c + \int_{\epsilon_0}^{\epsilon_{cf}} \epsilon_c f_c'' \left[1 - \frac{0.15}{0.004 - \epsilon_0} (\epsilon_c - \epsilon_0) \delta \epsilon_c \right]}{\epsilon_{cf} \int_0^{\epsilon_0} f_c'' \left[\frac{2\epsilon_c}{\epsilon_0} - \left(\frac{\epsilon_c}{\epsilon_0} \right)^2 \right] \delta \epsilon_c + \epsilon_{cf} \int_{\epsilon_0}^{\epsilon_{cf}} f_c'' \left[1 - \frac{0.15}{0.004 - \epsilon_0} (\epsilon_c - \epsilon_0) \delta \epsilon_c \right]} \\ &= 1 - \frac{\left[\frac{2\epsilon_c^3}{3\epsilon_0} - \frac{\epsilon_c^4}{4\epsilon_0^2} \right]_0^{\epsilon_0} + \left[\frac{\epsilon_c^2}{2} - \frac{0.15\epsilon_c^2}{2(0.004 - \epsilon_0)} \frac{(\epsilon_c - \epsilon_0)^2}{2} \right]_{\epsilon_0}^{\epsilon_{cf}}}{\epsilon_{cf} \left[\frac{\epsilon_c^2}{\epsilon_0} - \frac{\epsilon_c^3}{3\epsilon_0^2} \right]_0^{\epsilon_0} + \epsilon_{cf} \left[\epsilon_{cf} - \frac{0.15}{0.004 - \epsilon_0} \frac{(\epsilon_{cf} - \epsilon_0)^2}{2} \right]_{\epsilon_0}^{\epsilon_{cf}}} \\ &= 1 - \frac{\left[\frac{2\epsilon_0^2}{3} - \frac{\epsilon_0^2}{4} \right] + \left[\frac{\epsilon_{cf}^2}{2} - \frac{0.15\epsilon_{cf}^2}{2(0.004 - \epsilon_0)} \frac{(\epsilon_{cf} - \epsilon_0)^2}{2} \right] - \frac{\epsilon_0}{2}}{\epsilon_{cf} \left[\epsilon_0 - \frac{\epsilon_0}{3} \right] + \epsilon_{cf} \left[\epsilon_{cf} - \frac{0.15}{0.004 - \epsilon_0} \frac{(\epsilon_{cf} - \epsilon_0)^2}{2} \right] - \epsilon_0 \epsilon_{cf}} \end{aligned}$$

$$= 1 - \frac{\left[\frac{-e_0^2}{12} + \frac{e_{cf}^2}{2} - \frac{0.15e_{cf}^2}{2(0.004 - e_0)} \left(\frac{e_{cf}^2}{2} - e_{cf}e_0 + \frac{e_0^2}{2} \right) \right]}{\left[e_{cf}^2 - \frac{0.15e_{cf}}{0.004 - e_0} \left(\frac{e_{cf}^2}{2} - e_{cf}e_0 + \frac{e_0^2}{2} \right) \right] - \frac{e_{cf}e_0}{3}}$$

Therefore

$$\gamma = 1 - \frac{(e_{cf}^3 - 5.1e_0e_{cf}^2 - 0.004e_0^2 + 0.024e_{cf}^2)}{e_{cf}(3.925e_0^2 - 10.2e_0e_{cf} - 0.9e_{cf}^2 - 0.016e_0 + 0.048e_{cf})} \quad (3.21)$$

3.3.4 Location of Neutral Axis and Internal Resisting Moment:

The location of the neutral axis X was obtained from the equilibrium of internal forces across the depth of the cross section as given by equation 3.22. This equation is solved iteratively by first assuming a value for X . This was then varied until the equilibrium of forces across the depth of the cross section is satisfied, or the magnitude of the equation reached below some specified value.

$$\alpha f_c'' b x + \sum_{i=1}^n f_{si} A_{si} + f_{pl} A_{pl} - 0 \quad (3.22)$$

The internal resisting moment was obtained by summing the moments of all internal forces about the neutral axis, taking all and moment arms as positive quantities.

$$M = \alpha f_c'' b x \left(\frac{h}{2} - \gamma x \right) + \sum_{i=1}^n f_{si} A_{si} \left(\frac{h}{2} - d_i \right) + f_{pl} A_{pl} \left(\frac{h}{2} - d_{pl} \right) \quad (3.23)$$

3.3.5 Applied Load:

The applied load, P, was calculated by equating the internal resisting moment and the external moment produced by the applied load. For a simply supported slab with one concentrated load at the centre the external moment is given by:

$$M_{\text{ext}} = \frac{PL}{4} = M \quad (3.24)$$

solving for P;

$$P = \frac{4M}{L} \quad (3.25)$$

3.3.6 Curvature:

The curvature at midspan was calculated by dividing the concrete strain ϵ_{cf} by the neutral axis X

$$\phi = \frac{\epsilon_{cf}}{X} \quad (3.26)$$

3.3.7 Deflection:

The moment-area method was used to calculate the deflection of the simply supported, centrally loaded slabs that were tested in this study. The deflection, Δ , at the midspan of the slab is obtained from:

$$\Delta = \frac{L^2}{12} \phi \quad (3.27)$$

A microcomputer program called PSLAB (Plated Slab) was developed to carry out the numerical calculations. The program was written in FORTRAN 77 (see appendix I). The results of the analytical models were compared with experimental data of strengthened slabs.

3.4 Comparison of Measured and Analytical Results

This section describes the use of analytical models for the prediction of the ultimate response of the strengthened slabs in this study. The tables presented show the characteristics of the test slabs, the measured and analytical ultimate loads and moments along with the ultimate deflections as well as the mode of collapse of each slab. Finally, a discussion of the results follows with the aim of evaluating the correlation between the analytical and experimental data.

Using the data presented in Table 3.1 and the computer program PSLAB (see appendix A) written to solve the analytical models developed in this study, the ultimate behaviour for each strengthened slab was calculated. The comparison of the measured versus analytical values are presented in Tables 3.2 and 3.3. The modes of collapse observed during test included:

- (1) Concrete crushing due to Flexural-Punching,
- (2) Shear failure due to diagonal tension and
- (3) Plate separation before the crushing of concrete.

Because the analytical model assumed that the composite slabs have sufficient shear resistance to preclude diagonal tension failure, shear failure was not accounted for in PSLAB. Failure modes that were included are modes (1) and (3) listed above. The observed and predicted results on the modes of collapse are presented in Table 3.5.

Table 3.1 Geometrical and Material Properties of each Slab Series

Series No.	Slab No.	Concrete		Steel Reinforcements			Steel Plate / Epoxy Adhesive						Slab	
		f_c^c (N/mm ²)	ϵ_c^c (mm/mm)	t	d^i (mm)	A^i (mm ²)	t^p (mm)	b^{pl} (mm)	A^{pl} (mm ²)	f^a (N/mm ²)	E^a-E^s (N/mm ²)	B (mm)	H (mm)	
A	R0P0	35	0.0035	-	-	-	-	-	-	-	-	1000	100	
	R1P0	35	0.0035	-	-	-	-	-	-	-	-	1000	100	
B	R1EP	35	0.0035	1	88.63	478	3	700	2100	30	2500	1000	100	
	R1P2	35	0.0035	2	76.11	478	2	700	1400	400	200000	1000	100	
	R1P3	35	0.0035	2	76.17	478	3	700	2100	400	200000	1000	100	
	R1P4	35	0.0035	2	76.22	478	4	700	2800	400	200000	1000	100	
C	R0P2	35	0.0035	1	-	-	2	700	1400	400	200000	1000	100	
	R0P3	35	0.0035	1	-	-	3	700	2100	400	200000	1000	100	
	R0P4	35	0.0035	1	-	-	4	700	2800	400	200000	1000	100	
D	R1EP-P	35	0.0035	1	88.63	478	3	700	2100	30	2500	1000	100	
	R1P2-P	35	0.0035	2	76.11	478	2	700	1400	400	200000	1000	100	
	R1P3-P	35	0.0035	2	76.17	478	3	700	2100	400	200000	1000	100	
	R1P4-P	35	0.0035	2	76.22	478	4	700	2800	400	200000	1000	100	

3.4.1 General Observation on Measured and Predicted Results

The experimental and predicted ultimate loads and deflections are shown and compared in Table 3.2. The results show that the ratio of the measured and the calculated load capacities varies significantly even within the same series. These ratios across the series range from 0.64 to 1.26. However, the analytical values of almost all the slabs are within a reasonable approximation from the experimental ultimate load values and the agreement between these values is satisfactory. For the ultimate deflections of the test slabs, the calculated values in most cases (except in the case of slabs R1EP, R0P2 and R1EP-P) were marginally smaller than the test data as would be expected. The discrepancy can be attributed to a lower values of modulus of elasticity of concrete and much higher concrete ultimate strain (beyond the assumed value of 0.0035) in the slabs. The high crushing strain could have resulted from the confinement provided by the steel bearing plate transferring the load to the slab.

Table 3.2 Measured and Calculated Results for Slab Tests Series (A) through (D)

Series No.	Slab No.	Experimental Ultimate		Calculated Ultimate		Ratio of Experimental to Calculated	
		Load (kN)	Deflection (mm)	Load (kN)	Deflection (mm)	Load	Deflection
A	R0P0	39	2.33	35	1.96	1.11	1.89
	R1P0	122	9.81	105	5.78	1.16	1.70
B	R1EP	177	4.18	170	5.55	1.04	0.75
	R1P2	224	4.81	194	4.19	1.16	1.15
	R1P3	237	4.36	238	3.28	1.00	1.33
	R1P4	240	3.81	251	3.21	0.96	1.19
C	R0P2	233	4.04	185	4.62	1.26	0.88
	R0P3	165	4.07	235	3.39	0.70	1.20
	R0P4	161	4.00	252	3.24	0.64	1.24
D	R1EP-P	153	3.59	170	5.55	0.90	0.65
	R1P2-P	216	4.72	194	4.19	1.11	1.23
	R1P3-P	241	4.13	238	3.28	1.01	1.26
	R1P4-P	210	3.75	251	3.21	0.84	1.17

To find the average deflection and ultimate load approximation within each series, the mean deflection and load ratios of all slabs within the same series were calculated and presented in Table 3.3. The mean deflection ratios ranged from 1.078 to 1.795, while the ultimate load ratios ranged from 0.867 to 1.135. However, the percentage error of these mean deflection and load ratios from the exact mean ratio (assumed as 1.00) for series B to D ranged from 7.8% to 10.70% and -13.3% to 4.0% respectively. In the same comparison, series A has a mean deflection ratio of 79.5 and an ultimate load of 1.79. This fact shows again that PSLAB's accuracy could be considered good for the slabs of series B to D and not acceptable for series A.

Table 3.3 Mean Values of Deflection and Ultimate Load Ratios for each Slab Series

Series No.	Mean Ratio of Measured/Calculated		% Error	
	Load	Deflection	Load	Deflection
A	1.135	1.795	13.5	79.5
B	1.040	1.105	4.0	10.5
C	0.867	1.107	-13.3	10.7
D	0.965	1.078	-3.5	7.8

The ultimate flexural moments and plate strains of all the plated slabs were also calculated by the models developed and the results were compared with the experimental data and presented in Table 3.4.

The first thing to note in Table 3.4 is that the plate strains were in reasonably close agreement with the test data. The experimentally measured and theoretically computed ultimate moments of both plated and unplated slabs indicated that their mean ratio was about 1.00, with a minimum value of 0.64 and a maximum of 1.26. The relation between the measured and calculated ultimate moments was also studied in Fig. 3.5. The line of equality in the figure is labelled as 45-degree line. Had the calculated and the measured results been in perfect agreement, all the points would have been on the 45-degree line shown in the Fig. 3.5. The points which are below the line represent cases in which the actual moment exceeded the predicted value. The analytical results for these cases are, of course, conservative. The points above the 45-degree line represent an overestimation of the moments. It can be seen that all the points were relatively close to the 45-degree line and that the majority of the estimated results were conservative. In all cases, the predicted values compared very well with the limited experimental data.

Table 3.4 Ultimate Plate Strains and Moment Capacity of Test Slabs

Series No.	Slab No.	Ultimate Plate Strain (μ strain)		Ultimate Moment (kNm)		Ratio of Measured to Theoretical	
		Measured	Theoretical	Measured	Theoretical	Strain	Moment
A	R0P0	-	-	17.55	15.75	-	1.11
	R1P0	-	-	54.90	47.25	-	1.16
B	R1EP	-	-	79.65	76.50	-	1.04
	R1P2	668	600	100.80	87.44	1.11	1.15
	R1P3	540	500	106.65	107.03	1.08	1.00
	R1P4	528	500	108.00	112.81	1.06	0.96
C	R0P2	866	700	104.85	83.33	1.24	1.26
	R0P3	404	500	74.25	105.90	0.81	0.70
	R0P4	314	500	72.45	113.23	0.63	0.64
D	R1EP-P	-	-	68.85	76.50	-	0.90
	R1P2-P	752	600	97.20	87.45	1.25	1.11
	R1P3-P	562	500	108.45	107.03	1.12	1.01
	R1P4-P	420	500	94.50	112.80	0.84	0.84

mean ratio = 1.00

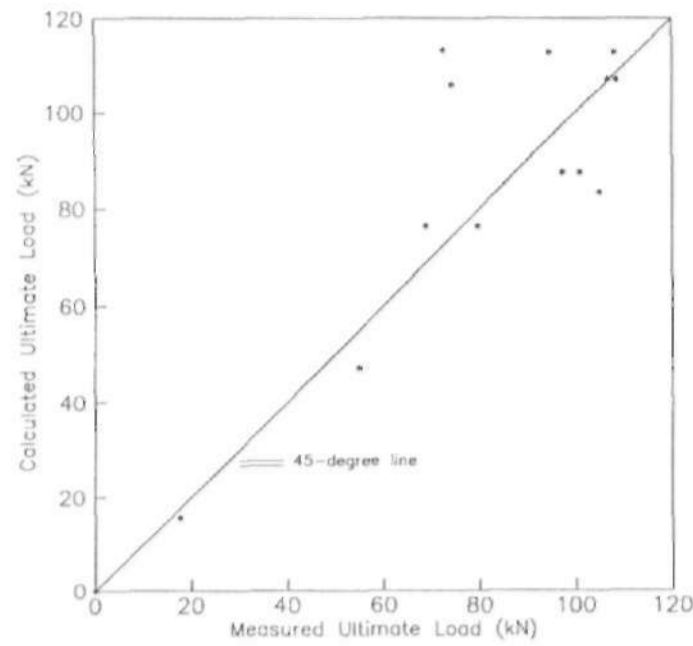


Fig. 3.5 Comparison of Measured and Predicted Ultimate Moments

The expected (i.e. from calculations) and actual modes of failure of the test slabs are given in Table 3.5. The results show that the analytical models can to a very large extent predict the modes of collapse of strengthened slabs. Plated slabs can fail in several ways when loaded in bending. Failure modes observed in slabs tested in this study can be classified into three categories: Flexural-Punching failure, Shear failure and Plate Separation. Flexural-Punching takes place in slabs in which most of the reinforcement yields before punching occurs and consequently the slab exhibits large deflections prior to failure. Shear failure occurs when the slab shows small deflections, with yielding of the

tension steel being very localised at the point of load application. Plate Separation can occur due to:

- (1) the sudden propagation of cracks in the adhesive (most resin adhesives are brittle);
- (2) peeling-off of the steel plate because of the shear cracks in the concrete; and
- (3) shear failure of the concrete layer between the steel plate and the longitudinal reinforcement.

Slab ROP0 of series (A) failed in pure shear as predicted and so did the slabs of series (c). Slab R1P0 of series (A) and all the slabs of series (B) and (D) were expected to fail in flexure, these slabs (except slab R1P2) did so after the formation of the yield line patterns, and then, a punching failure occurred. However, slab R1P2 failed in flexural-punching after debonding due to the peeling-off of the steel plate. The peeling-off debonding takes place in the epoxy adhesive used to bond the steel plate to the concrete. This was observed to produce a sudden drop in the load-deflection curve at a point corresponding to the response of the slab after yielding of the steel reinforcement.

Although only test data from this study were used to evaluate the analytical models, it can be stated that the models are likely to yield satisfactory results for strengthened slabs in which shear failure is precluded.

Table 3.5 Comparison of Observed and Predicted Modes of Failure

Series No.	Slab No.	Observed Mode	Predicted Mode
A	R0P0	S	S
	R1P0	F	S
B	R1EP	F	F
	R1P2	P	F
	R1P3	F	F
	R1P4	F	F
C	R0P2	S	S
	R0P3	S	S
	R0P4	S	S
D	R1EP-P	F	F
	R1P2-P	F	F
	R1P3-P	F	F
	R1P4-P	F	F

Note: F = Flexure-Punching predominant concrete crushing

S = Shear or Punching shear predominant concrete rupture

P = Plate Separation

CHAPTER 4

EXPERIMENTAL INVESTIGATIONS**4.1 Materials**

All the materials used in these tests were tested and found to comply with the requirements of the relevant standards. They were also obtained from a single source in to order minimise any difference in properties. The materials are enumerated here under.

4.1.1 Concrete

The concrete in the slabs was designed for a 28-day compressive strength of about 35 N/mm² consistent with that used in precast prestressed beams in bridge construction. The mix proportions were 1:1.8:1.9 (Cement:Fine Aggregates:Coarse Aggregates) with a water/cement ratio of 0.52 and containing a plasticiser for adequate workability. High early strength cement, two types of coarse aggregates with maximum sizes of 12.5 mm and 7 mm, and fine aggregates of silica sand (size passing 0.5 mm) were used. The mixes were designed to have a slump of 100 mm. The mix details are given in Table 4.1. Six concrete cylinders 152 mm in diameter and 305 mm high per slab were cast, cured under the same curing conditions as the test slabs and tested the day that a corresponding slab was tested. The mix was vibrated with electronic vibrators in forms and the cylinders and slabs were cured for at

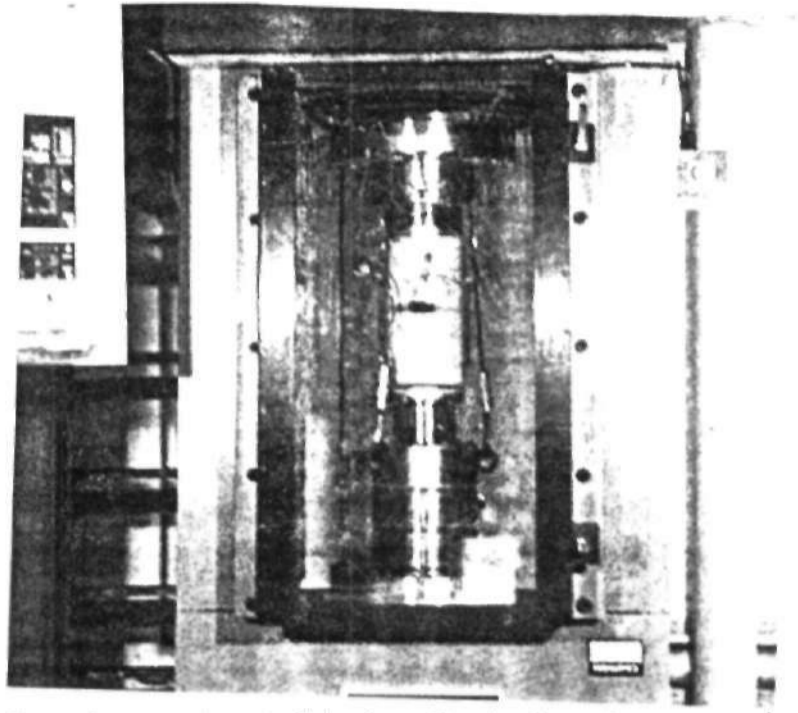


Plate I Concrete Cylinder Test for Compressive Strength

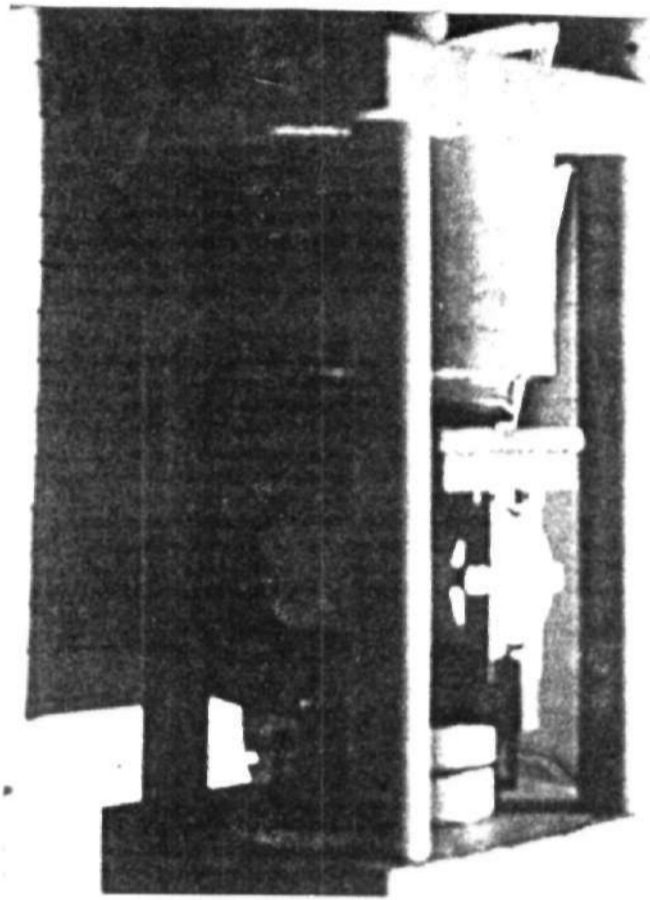


Plate II Split-Cylinder Test for Concrete Tensile Strength

Table 4.2 summarizes the measured mechanical properties of the concrete. The compressive strain at maximum compressive concrete stress and tensile strain at the maximum tensile stress are also given in Table 4.2. Typical concrete stress-strain curve is shown in Figure 4.1. The compressive strength was calculated by dividing the maximum load by the cross sectional area of the cylinder. The tensile strength was calculated from:

$$f_r = \frac{2P}{\pi LD} \quad (4.1)$$

where:

- f_r = tensile strength
- P = maximum applied load
- L = specimen length
- D = specimen diameter

The modulus of elasticity was calculated using the following equation as given in ACI 318-83 (ACI, 1983):

$$E_c = 0.043W_c^{1.5}\sqrt{f'_c} \quad (4.2)$$

where:

- E_c = modulus of elasticity (N/mm²)
- W_c = unit weight (kg/m³)
- f'_c = compressive strength (N/mm²)

Table 4.2 Mechanical Properties of Concrete

Test Sample	Compressive Strength (N/mm ²)	Compressive Strain (x 10 ⁻³)	Tensile Strength (N/mm ²)	Tensile Strain (x 10 ⁻⁴)	Modulus of Elasticity, E _c (N/mm ²)
R0P0	37.71	3.0	3.44	1.08	30700
R1P0	40.56	2.7	3.57	1.09	31840
R1EP	39.05	2.8	3.50	1.07	31250
R1P2	41.29	2.6	3.60	1.10	32130
R1P3	40.65	2.5	3.57	1.08	31880
R1P4	37.49	2.9	3.43	1.09	30620
R0P2	42.59	2.5	3.66	1.08	32630
R0P3	38.27	2.9	3.46	1.07	30930
R0P4	40.50	2.7	3.56	1.09	31820
R1EP-P	39.42	3.0	3.52	1.06	31390
R1P2-P	40.68	2.6	3.57	1.07	31890
R1P3-P	44.73	2.5	3.75	1.12	33440
R1P4-P	41.12	2.6	3.59	1.08	32060

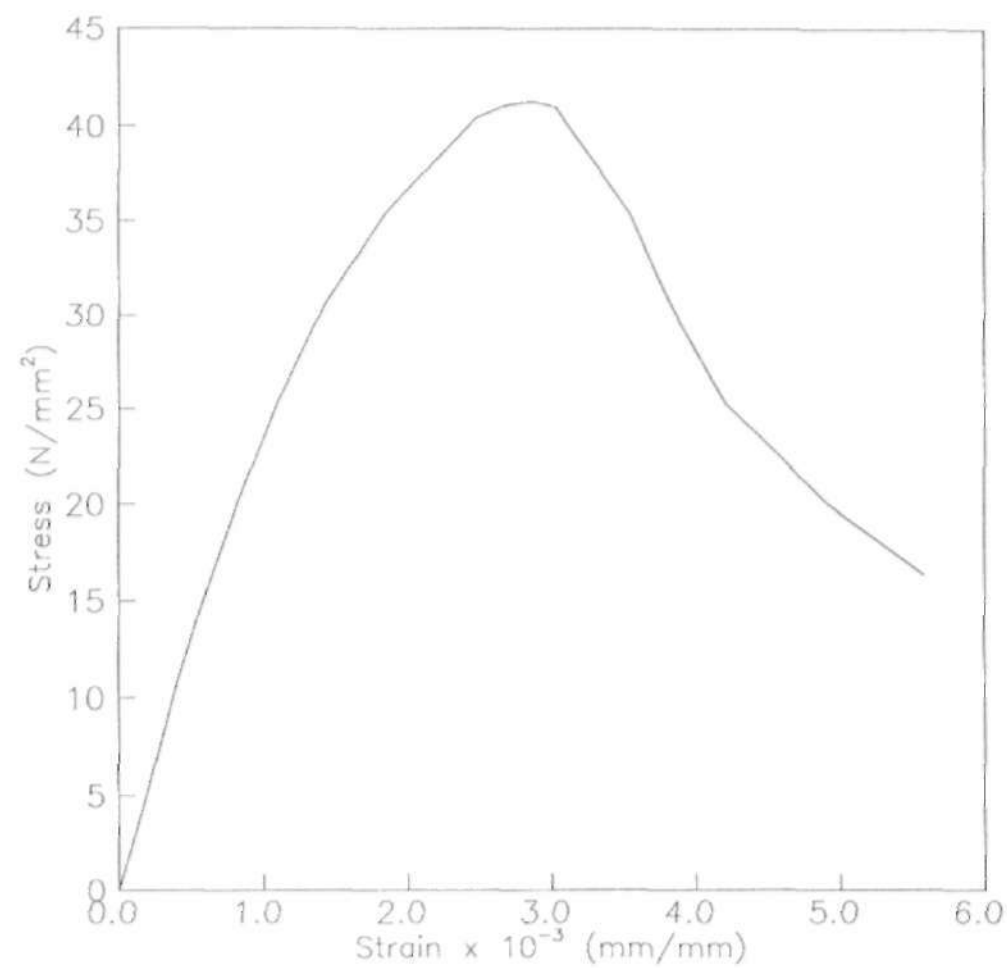


Fig. 4.1 Typical Stress-Strain Curve for Concrete Cylinders Loaded in Uniaxial Compression

4.1.2 Steel Reinforcement

Cold-worked deformed bars conforming to the requirements of ASTM A588 (ASTM, 1973) and BS 4461 (BS, 1969) standards for deformation were used as tension steel in all the slabs. The steel was of high yield material with a diameter of 4.04mm. Six control specimens of the reinforcing steel were cut and tested at a cross-head speed of 25mm/min under uniaxial tension to establish their yield and ultimate strengths. A 50mm extensometer was used to determine the steel strains (see plate III).

The measured tensile properties, given in Table 4.3, exceeded, the minimum yield stress (517 N/mm^2), tensile strength (586 N/mm^2) and elongation (16 percent), specified in ASTM A588 (ASTM, 1973). A typical uniaxial stress-strain curve for the steel bars in tension is shown in Fig. 4.2.

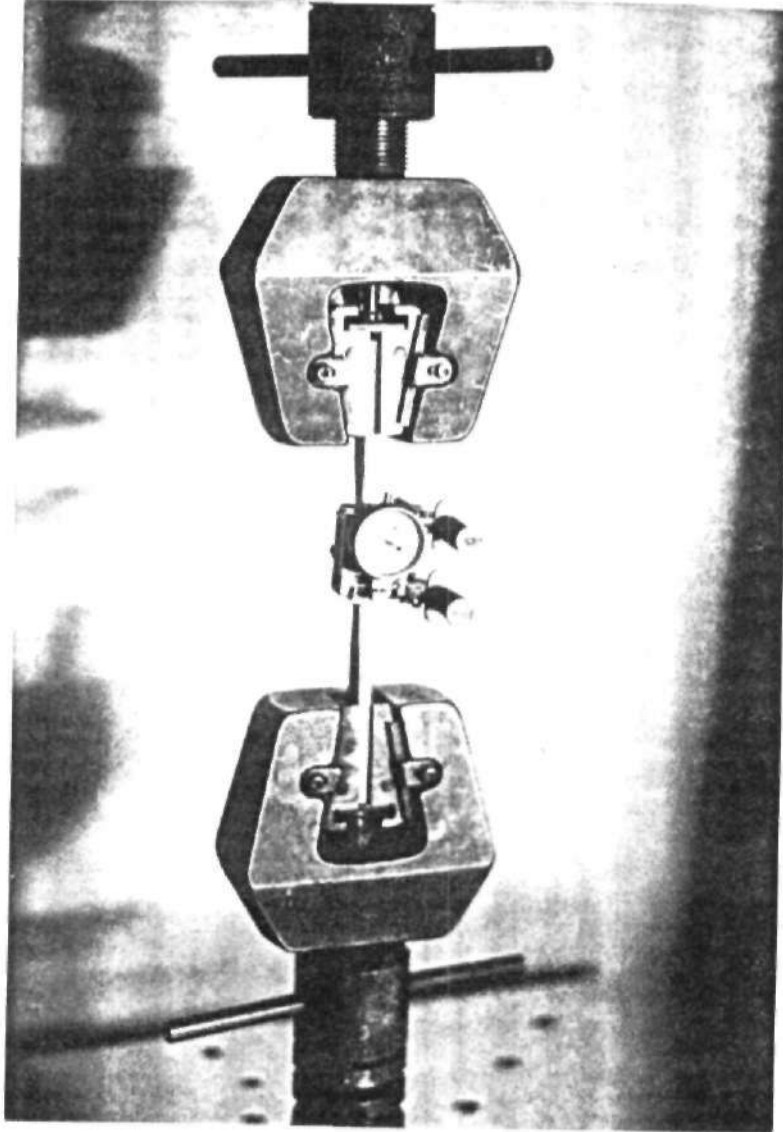


Plate III Steel Uniaxial Tension Test

Table 4.3 Summary of Properties of Steel Plates and Reinforcing Bar

Sample	Proof/Yield Stress (N/mm ²)	Ultimate Strength (N/mm ²)	Gauge Length (mm)	Elongation (%)	Elastic Modulus (kN/mm ²)
2 mm Plate	317.87	401.73	195	24	210
3 mm Plate	360.79	464.84	195	22	210
4 mm Plate	403.71	527.00	195	20	210
4 mm bar	517.84	638.95	300	18	220

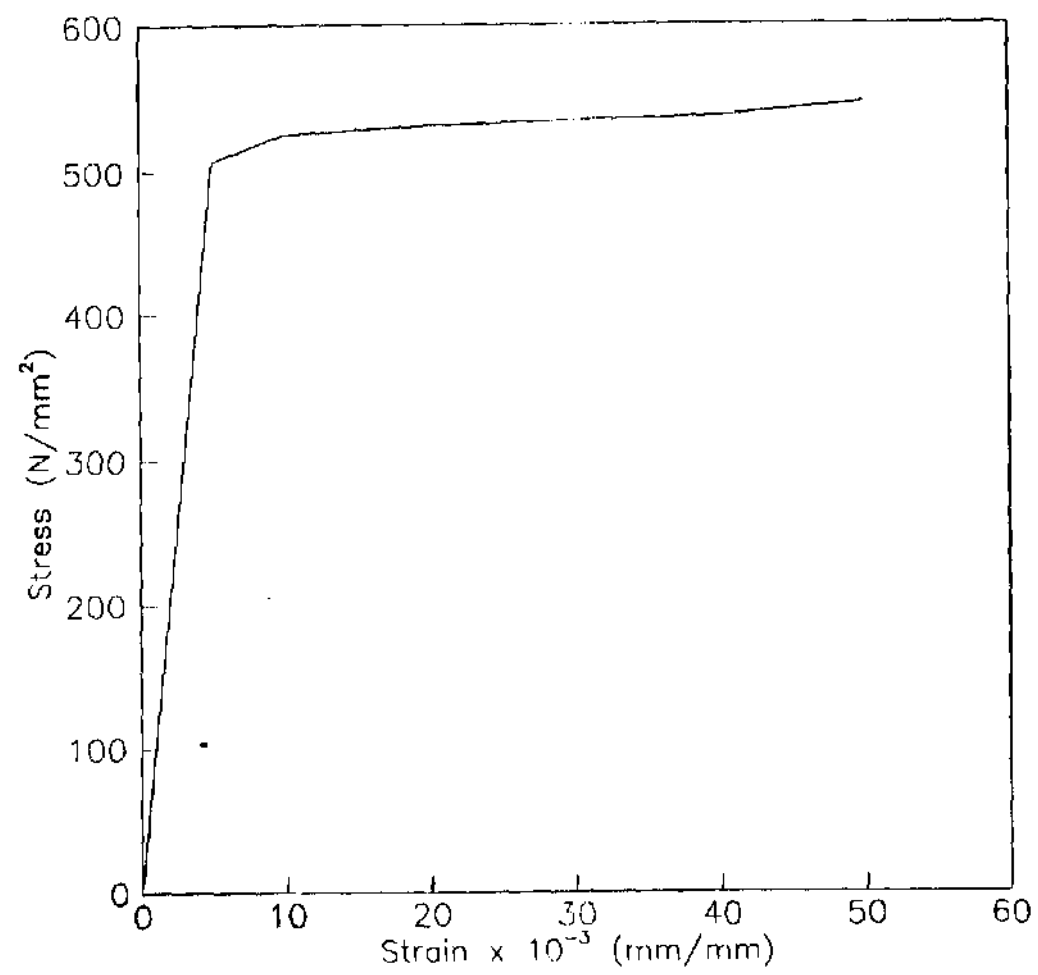


Fig. 4.2 Uniaxial Stress-Strain Curve for Steel in Tension

4.1.3 Steel Plate

Three plate thicknesses of 2mm, 3mm and 4mm, were used as external reinforcement. Each plate was of mild steel meeting the requirements of BS 1449. As with steel bars, six samples were cut from each plate thickness to measure the yield and ultimate strengths. The 2mm, 3mm and 4mm plates had yield stresses of 318, 361 and 403 N/mm² and ultimate strengths of 402, 465 and 527 N/mm², respectively. The summary of their properties are also presented in Table 4.3.

4.1.4 Epoxy

The success of the plate bonding strengthening technique is critically dependent on the performance of the epoxy used. Numerous types of epoxies with a wide range of mechanical properties are commercially available. A most suitable epoxy for this particular application according to Mays and Hutchinson (1988) would be one that has sufficient strength and stiffness to resist interfacial shear stresses necessary to ensure structural composite action between the steel plate and concrete. At the same time, the epoxy should be tough to prevent brittle failure of bond between concrete and plate.

Proper design of epoxy-bonded joints requires an appreciation of the properties of the different materials to be joined as well as quantitative data on the properties of structural adhesives. Table 4.4 compares typical engineering properties of a cold-curing epoxy adhesive with those of concrete and mild steel. In joint design, full account must be taken of the poor resistance of adhesives to peel and to cleavage forces; shear strength itself is unlikely to be a limiting factor. This is overcome by the use of flexible or toughened epoxies. To limit the effects of creep under sustained load, an adhesive possessing a glass transition temperature well above the service temperature is required. The use of such an adhesive should also result in the improved environmental durability of a bonded assembly.

The epoxy resin used in the tests was Sikadur[®] 31, provided by Sika Limited, Canada; and was a two-part system with a paste-like consistency. The epoxy was used in accordance with the instructions by the manufacturer. According to the data supplied by the manufacturer, the lap shear strength of the epoxy with metal substrates ranged from 14 to 15 N/mm² with a maximum elongation at failure of 40 percent.

The required curing time of the epoxy was 4 hours at room temperature. It had a tensile strength of about 20 N/mm^2 , elastic modulus 2.5 N/mm^2 and poisson's ratio of 0.34. These properties are given in Table 4.5. The manufacturer also indicated that it had a very good resistance to salt and moisture.

Table 4.4 Comparison of Typical Engineering Properties of Epoxy, Concrete and Mild Steel

Property (at 20°C)	Cold-curing Epoxy Adhesive	Concrete	Mild steel
Relative density	1.3	2.2	7.8
Young modulus: GNm^{-2}	4	30	210
Shear modulus: GNm^{-2}	1.4	10	80
Poisson's ratio	0.37	0.18	0.29
Tensile strength: MNm^{-2}	25	4	400
Shear strength: MNm^{-2}	30	5	550
Compressive strength: MNm^{-2}	75	40	400
Tensile elongation at break: %	0.5-5	0.15	30
Approximate work of fracture: Jm^{-2}	100	20	10^5-10^6
Linear coefficient of thermal expansion, per $^\circ\text{C}$	35	10	11
Water absorption 7 days at 25°C : % w/w	1	5	
Glass transition temperature: $^\circ\text{C}$	45		

Table 4.5 Typical Properties of Epoxy Adhesive used

Property	Value
Elastic Modulus (kN/mm ²)	1.5 to 3.0
Lap Shear Strength (N/mm ²)	15 to 30
Tensile Strength (N/mm ²)	15 to 90
Flexural Strength (N/mm ²)	10 to 100
Compressive Strength (N/mm ²)	100 to 175
Tensile Elongation (%)	3 to 50
Poisson's Ratio	0.25 to 0.40
Curing Time (hrs)	3 to 10

4.2 Test Specimens

Four series of square concrete slabs, totalling 13 slabs were tested to failure in this study. The dimensions and reinforcement details of a typical test specimen are given in Fig. 4.3. Full details of the test slabs are given in Tables 4.6 and 4.7 and typical design calculations are in appendix II.

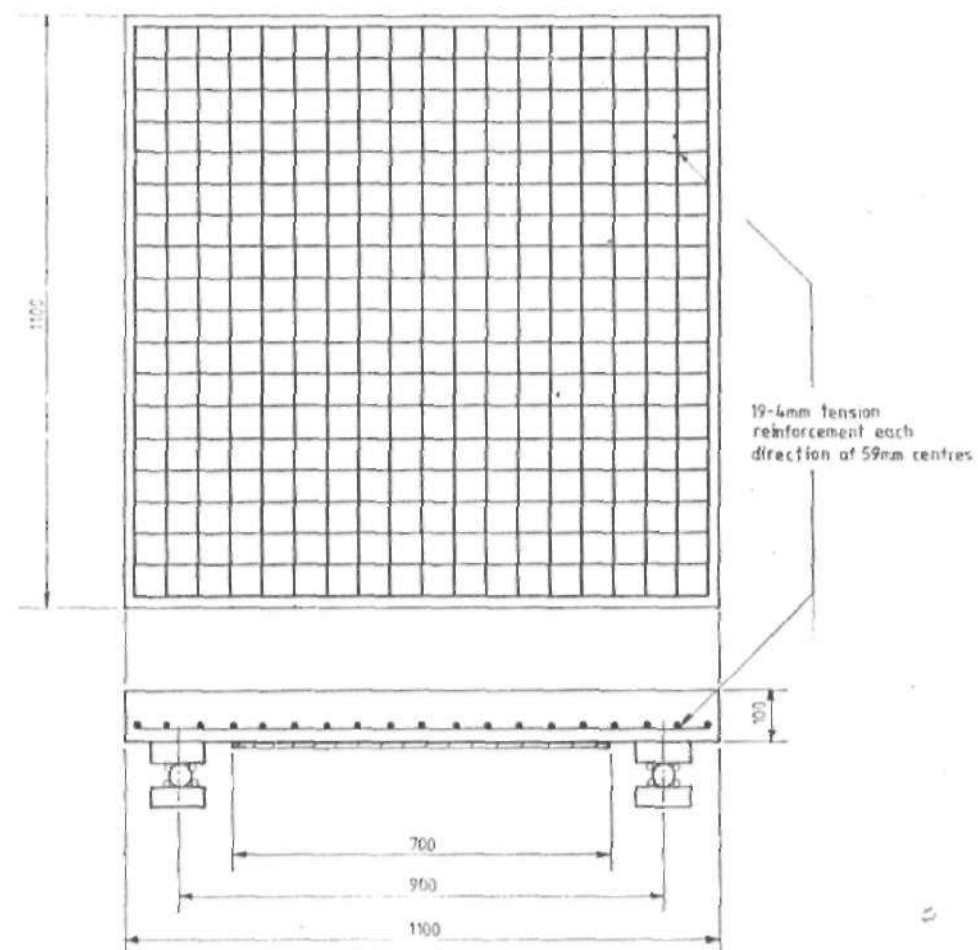


Fig. 4.3 Dimensions of a Typical Test Slab and Reinforcing Details

In a series, each slab is identified with an acronym, where the first two symbols indicate whether the slab is internally reinforced or not. R0 means no internal reinforcement, (i.e. $\rho = 0$); R1 means tension reinforcement is provided (i.e. $\rho = 0.708$). The next two symbols indicate whether epoxy glue or steel plate is used to strengthen the slab. EP, P2, P3 and P4 stands for

Table 4.6 Details of Test Slabs

Series No.	Slab No.	Average Concrete Compressive Strength (N/mm ²)	Bar Size (mm)	Bar Spacing (mm)	Steel Ratio ρ (%)	Bonded Steel Plate Thickness (mm)	Cross-Sectional Area of Plate (mm ²)	Slab Thickness (mm)	% Load before Plating
A	ROP0	37.71	-	-	-	-	-	100	-
	R1P0	40.56	4	59	0.708	-	-	100	-
B	R1EP	39.05	4	59	0.708	E ¹	EA ¹¹	100	-
	R1P2	41.29	4	59	0.708	2	1400	100	-
	R1P3	40.65	4	59	0.708	3	2100	100	-
	R1P4	37.49	4	59	0.708	4	2800	100	-
C	ROP2	42.59	-	-	-	2	1400	100	-
	ROP3	38.27	-	-	-	3	2100	100	-
	ROP4	40.50	-	-	-	4	2800	100	-
	R1EP-P	39.42	4	59	0.708	E ¹	EA ¹¹	100	45
D	R1P2-P	40.68	4	59	0.708	2	1400	100	40
	R1P3-P	44.73	4	59	0.708	3	2100	100	40
	R1P4-P	41.12	4	59	0.708	4	2800	100	40

Note: E - 3 mm thick Epoxy Layer
EA - 2100 mm² Epoxy Area

3mm thick epoxy layer, 2mm, 3mm and 4mm thick steel plate respectively. The last symbol P indicates that the slab was preloaded to first crack load. The test series comprised the following:

4.2.1 Series A

Two slabs were tested in this series. These are R0P0 and R1P0. They were 1.10m x 1.10m in overall area, while the clear span was 0.90m in each direction. They were simply supported on all four sides and load was transmitted to the centre of each slab through a ball-joint on 170mm dia. x 50mm long steel bar. Slab R0P0 had no reinforcement or steel plate but slab R1P0 was reinforced with a 4mm deformed bar at its bottom and had no plate. The slabs in this series were used as reference slabs.

4.2.2 Series B

Four slabs were tested in this series. They included R1EP, R1P3, R1P2, R1P3 and R1P4. Each slab had properties similar to slab R1P0 of series A except that a 3 mm thick epoxy layer, 2 mm, 3 mm and 4 mm thick steel plate was bonded to the tension face of R1EP, R1P2, R1P3 and R1P4 respectively. Each steel plate and adhesive layer was 700 mm x 700 mm in area. The slabs were loaded in a manner identical to series A, previously described. This series was

intended to simulate an unsatisfactory structural behaviour of reinforced concrete slabs existing in certain buildings.

Table 4.7 Details of Strengthening

Series No.	Slab No.	Strengthening
A	R0P0	Plain Concrete Slab (No reinforcement no Plate)
	R1P0	Reinforced Concrete Slab (No Plate)
B	R1EP	As R1P0 + 3 mm thick epoxy layer
	R1P2	As R1P0 + 2 mm steel plate
	R1P3	As R1P0 + 3 mm steel plate
	R1P4	As R1P4 + 4 mm steel plate
C	R0P2	As R0P0 + 2 mm steel plate
	R0P3	As R0P0 + 3 mm steel plate
	R0P4	As R0P0 + 4 mm steel plate
D	R1EP-P	As R1P0 + precracked and 3 mm layer of epoxy
	R1P2-P	As R1P0 + precracked and 2 mm steel plate
	R1P3-P	As R1P0 + precracked and 3 mm steel plate
	R1P4-P	As R1P0 + precracked and 4 mm steel plate

4.2.3 Series C

Three slabs were tested to failure in this series. Their geometrical properties were generally identical to that of slab R0P0 of series A except that a 2 mm, 3 mm and 4 mm thick steel plate was epoxy-bonded to the tension face of R0P2, R0P3

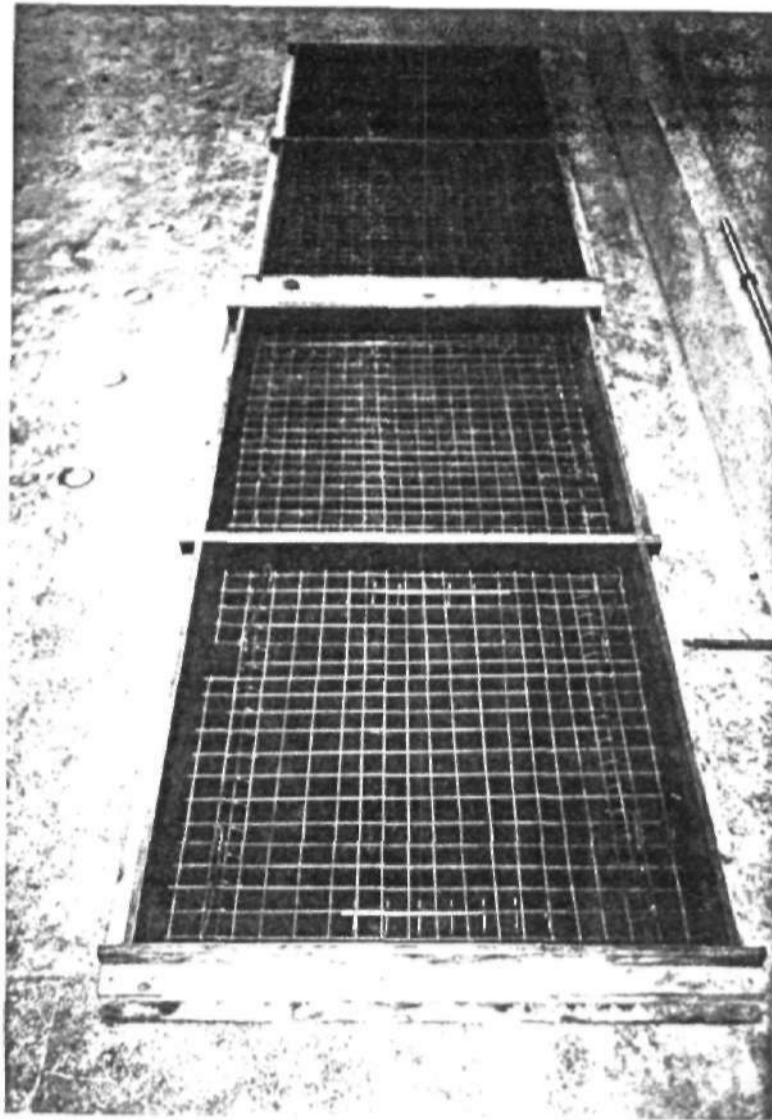


Plate IV Reinforcement Pattern for Test Slabs

4.4 INSTRUMENTATION

The slabs were extensively instrumented. The strains in the plates were measured by electric resistance strain gauges ERS at several locations in the lateral and diagonal directions as shown in Fig.

4.4. The gauges were Japanese foil ERS gauges, FKL, 120 Ω , 5mm gauge length. Deflection was monitored through linear variable differential transformers LVDTs placed on the top of the slab at midspan and in the lateral directions. In addition, slip at interface between plate and concrete was also measured by LVDTs placed at two ends. Load was measured by a load cell. The averages of the measured strains, deflections and slips were used in the analysis of data.

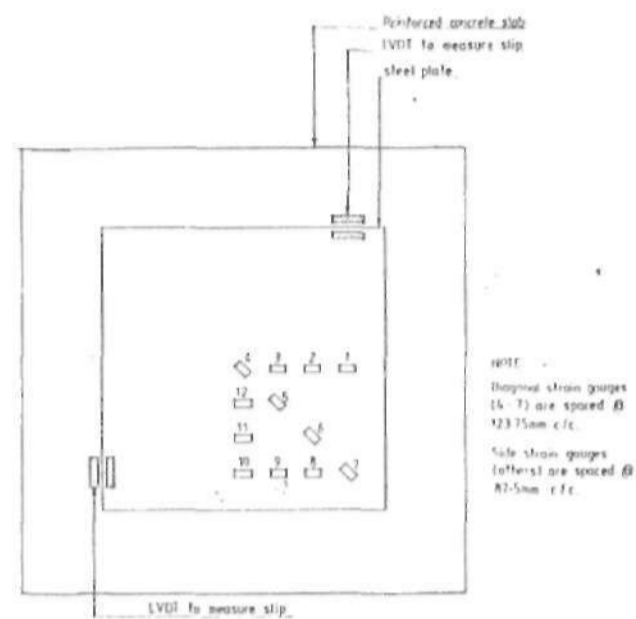


Fig. 4.4 Electrical Strain Gauges Locations

4.5 TEST EQUIPMENT AND PROCEDURE

All slabs were cast, strengthened and tested in the Civil Engineering and Applied Mechanics Laboratory of the McGill University, Montreal, Canada. For

convenience in conducting the slab tests, a special steel frame was constructed. The frame was placed under the testing machine, as shown in plate V. All the test slabs were simply supported along four edges on a clear span of 0.90 m and they were centrally loaded. The load was applied through a ball-joint on a solid high tensile bar 170mm dia. x 50mm long. Layers of rubber contained within a bar were used to help distribute the load uniformly to the specimens. The tests were carried out using a universal testing machine with a maximum capacity of 670 kN. Load was applied to the specimens at an approximately constant rate up to the failure load. The test was stopped when the applied load decreased to about 0.75 times the ultimate load.

During testing, the slabs were carefully inspected and cracks were marked at each load increment. Deflection at the slab centres and other positions, steel plate strains and slip at interface between plate and concrete were taken at approximately 10 kN increments through an automatic data acquisition system. The phenomena of failure was also recorded.

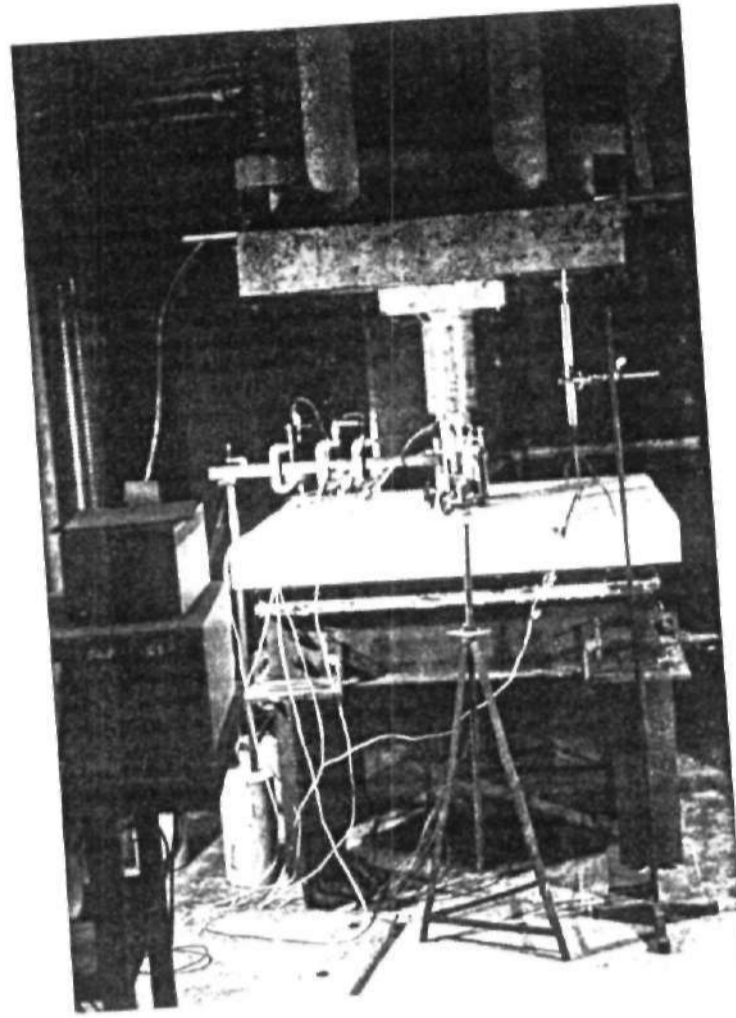


Plate V General View of Test Rig

4.6 Test Results and Discussion

It is recalled that one of the objectives of this study was to investigate the structural behaviour of plated concrete slabs (those that are significantly cracked). The results of tests conducted on some

materials used in this research have been presented in the previous chapter. The results presented in this chapter are those of the main tests performed on the thirteen (13) concrete slabs. The test procedure followed has been described above. For each set of slabs, extensive data on the characteristics of deformation, crack pattern, strength and modes of failure were obtained from these tests. The summary of the results are presented in Tables 4.8 to 4.12 and discussed below.

4.6.1 Deformation Properties

4.6.1.1 Deflection Behaviour

The measured load-deflection behaviour at the midspan of slab for all the test series are shown in Figs. 4.5 to 4.8. The deflections at the first crack and ultimate loads and their ratio in each series are summarised in Table 4.8 for comparative analysis. The data for series (A) show that the ratio of deflection for slab R1P0 at its ultimate load to its first crack load was 4.69 and that reinforcement and epoxy glue have a distinct effect on stiffening the structural member. The load-deflection character (Fig. 4.1) of the control unplated slab is compared with those of plated slabs. From the figures (4.5 to 4.8) it is generally observed that the stiffness of the plated slabs is enhanced at all the stages of loading.

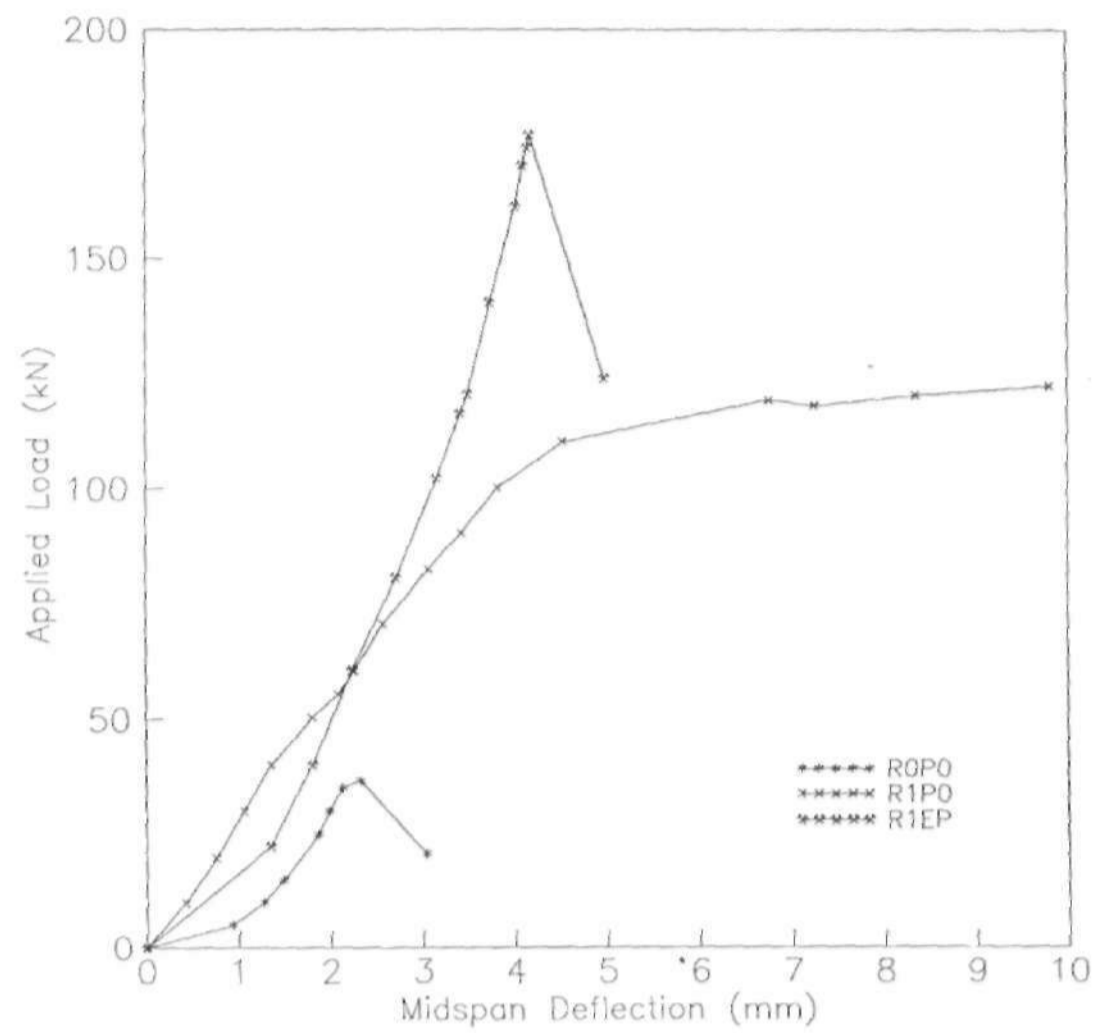


Fig. 4.5 Load - Deflection Curves for Slabs in Series A

For slabs in series (B), the deflection sustained by the unplated control slab R1P0 corresponding to its ultimate load of 122 kN was 9.81mm whereas the plated slabs R1P2, R1P3 and R1P4 had undergone a deflection of only 3.58mm, 3.07mm and 2.71mm respectively corresponding to this load. The ratio of ultimate to cracking deflections ranged from 1.12 to 1.22. The presence of epoxy adhesive

alone (as in slab R1EP) also reduced the deflection value by about 45 percent. Further, it was also observed that as the steel plate thickness increases, the reduction in deflection increased and the stiffening effect reduced.

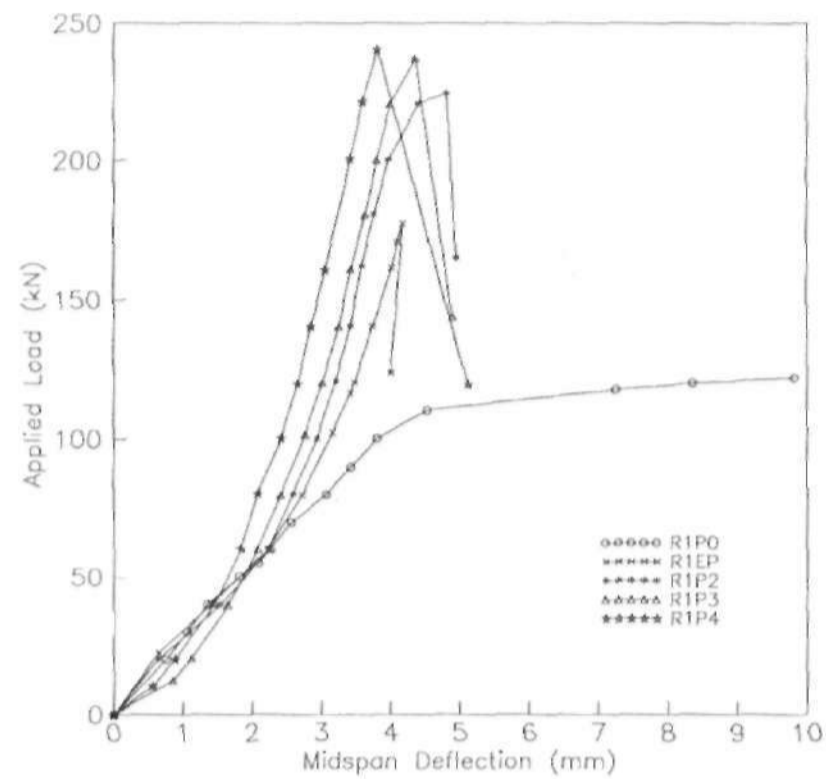


Fig. 4.6 Load - Deflection Curves for Slabs in Series B

The deflection behaviour for slabs in series (C) is more or less similar (Fig. 4.7). The plated slabs being more stiffer showed less deflections than the unplated slab. The stiffness of the slabs, however, reduced after the concrete cracked. The load-deflection then continued until failure. A drop in load from 154 kN to 123 kN was

observed in the case of slab R0P4. This could be attributed to slip and imperfect composite action at the bond between the plate and concrete. The deflections observed at failure loads were considerably lower in series (C) in comparison with the reference slab (i.e. series A).

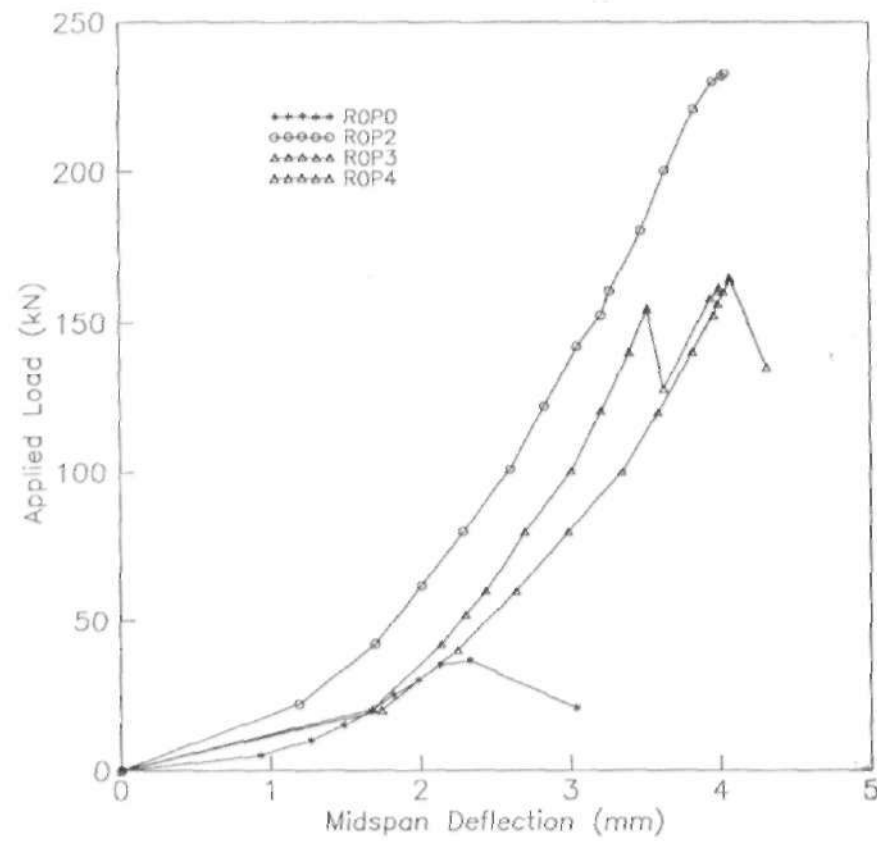


Fig. 4.7 Load - Deflection Curves for Slabs in Series C

Because the slabs in series (D) were preloaded, then unloaded, it was observed that they had some residual deflections on unloading. These slabs were then strengthened and reloaded before the residual deflections

were fully recovered. The unload-reload segment exhibited a small hysteresis loop but the loop closed at the same point at which the slabs had been unloaded. The loading was then continued until the slabs failed as a result of sudden failure as shown in plate VI. The deflection curves (Fig. 4.8) show that slabs in series (D) behaved like the unplated control slab R1P0 during preloading stage and like the plated slabs of series (B) after they were strengthened. It is also interesting to note that, even though extensively cracked prior to loading, slabs of series (D) exhibited slightly increased stiffness compared to the plated slabs of series (B) (Table 4.8), partly because of the filling of cracks by the glue. This increased stiffness was particularly obvious at loads higher than the previously applied loads.

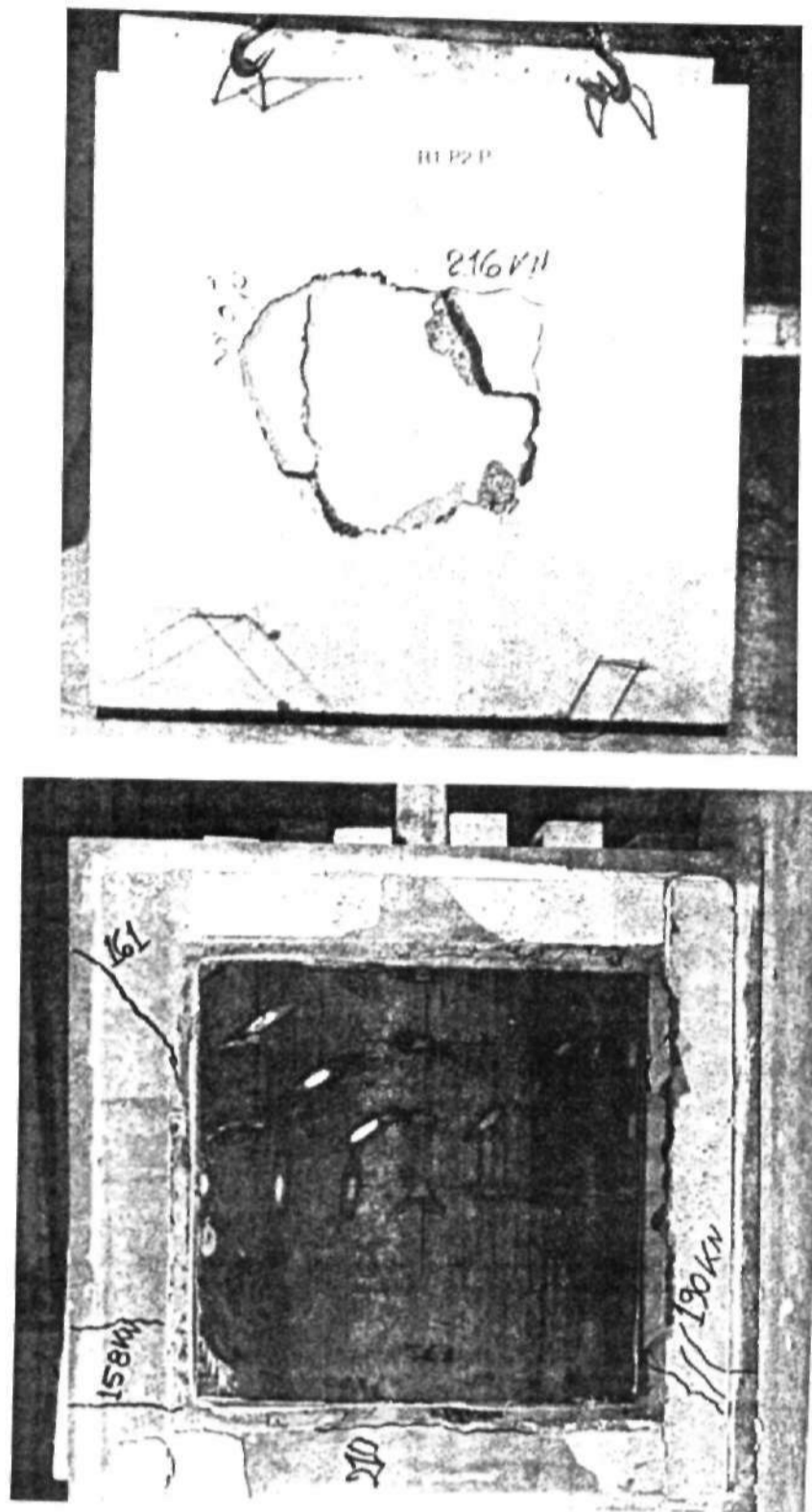


Plate VI Failure Patterns of Test Slabs in Series (A) through (D)

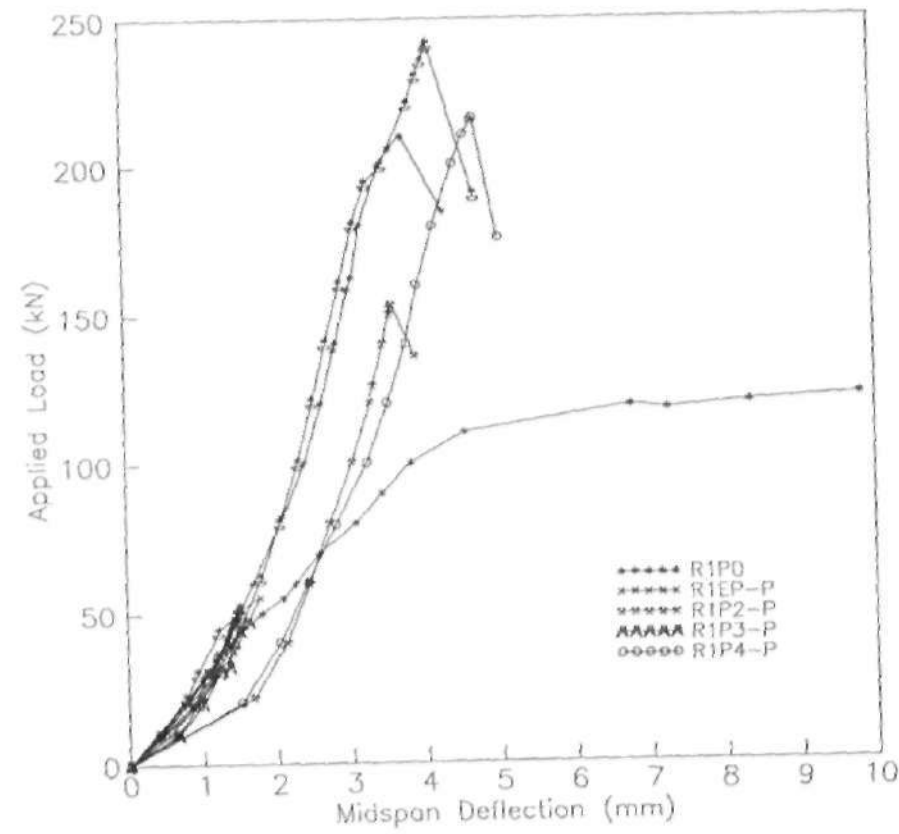


Fig. 4.8 Load - Deflection Curves for Slabs in Series D

4.6.1.2 Strain Deformations

Fig. 4.9 shows the applied load versus steel plate strain curves for slabs in series (B). The data show that the behaviour is approximately linear up to the cracking loads. After the cracking of concrete, the tension force in the concrete is transferred to the reinforcing bars and plate, resulting in higher strains. The load-strain curves continued until the bars yielded. At this point, the strains in the plate increased at a significantly higher rate, indicating that the plates alone further

carried the increments of the tensile components of the internal moments. The stiffening effect of the glued plates was observed to be more influential in reducing cracking than in reducing deflection. This is important from structural point of view; since the reinforcing bar strains control the crack width in the concrete; the steel plate provides a restraining medium to crack initiation and crack growth. From the crack control point of view, therefore, the plated and glued slab show far greater stiffness than an unplated slab.

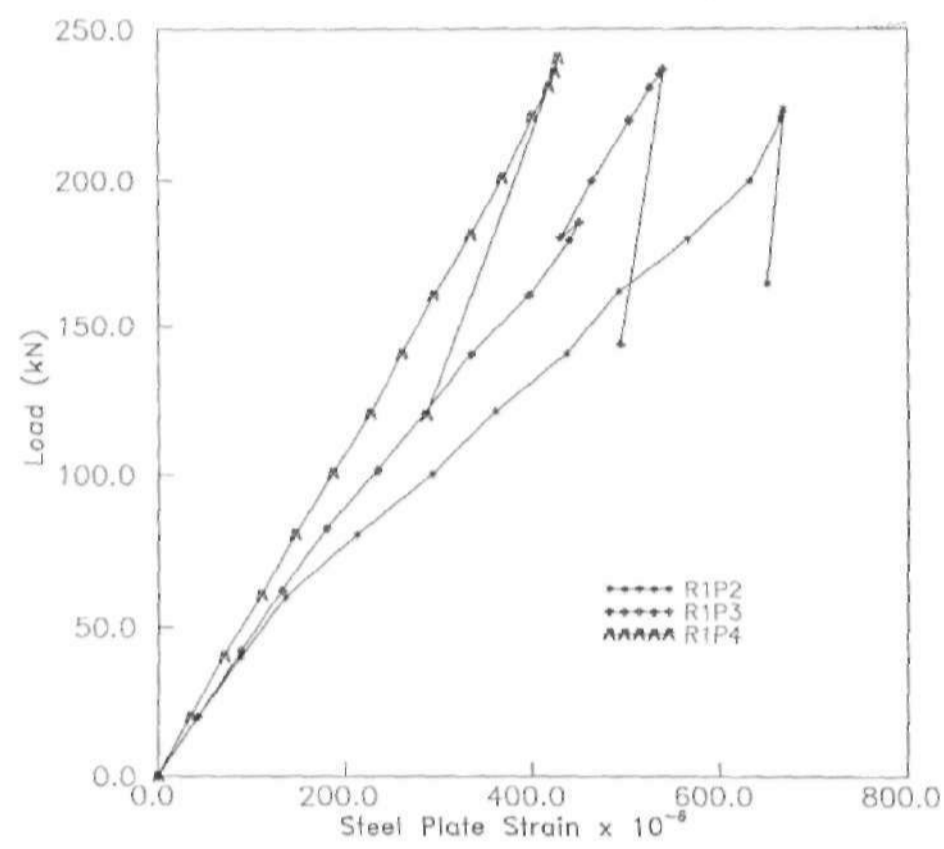


Fig. 4.9 Load versus Steel Plate Strain for Slabs in Series B

The steel plate strain distribution at the midspan during loading in slabs of series (C) was also monitored as in series (B). It can be seen from Fig. 4.10 that up to 154 kN, slabs ROP3 and ROP4 behaved similarly with linear response. The strain in slab ROP2 also increased roughly linearly up to a load of about 230 kN. A drop in load due to slip was observed in slab ROP4. After concrete cracking, the strain in the plate increased at much faster rate, indicating that the composite plate alone resisted the tensile component of the internal moment couple for further increases in the applied load. The rate of build-up of strains along the plates increases as the plate thickness is reduced.

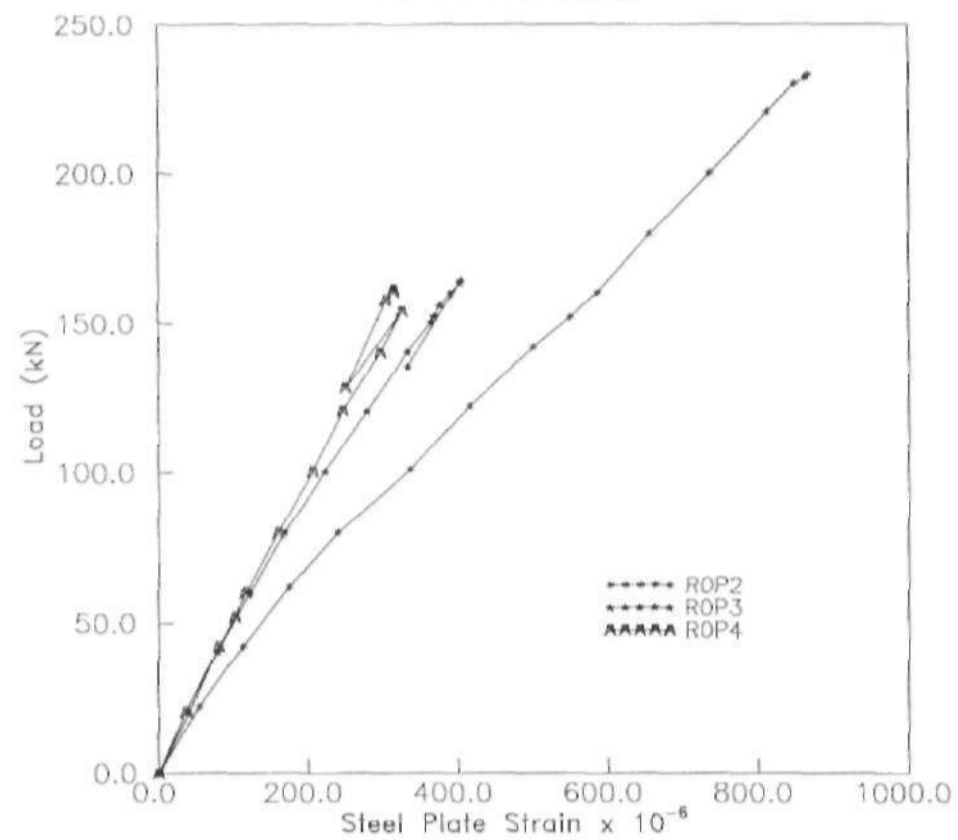


Fig. 4.10 Load versus Steel Plate Strain for Slabs in Series C

Fig. 4.11 illustrates the variation of plate strain in slabs of series (D). The results indicate that all the slabs in this series showed plate strain almost identical with those of series (B), confirming the effectiveness of the plating technique even in heavily cracked slabs. The load-strain character was initially linear up to cracking load. Following this load, the behaviour continued nonlinearly until failure occurred. The maximum plate strain recorded in this series was 752 μ strains (Table 4.9). This is 13 percent lower and 15 percent higher than the maximum values recorded in series (C) and (B) respectively. It was further observed that the maximum recorded strain decreased with increase in structural deformations prior to plating. This is clearly, understandable from the structural point of view. Nevertheless, the more important structural action to be recognised is the capability of the plating bonding operation in restoring the stiffness and strength conditions of even the damaged slabs better than the original undamaged slab.

Table 4.9 Measured Ultimate Plate Strains of Test Slabs

Series No.	Slab No.	Ultimate Plate Strain (μ strains)
A	R0P0	-
	R1P0	-
B	R1EP	-
	R1P2	668
	R1P3	540
	R1P4	528
C	R0P2	866
	R0P3	464
	R0P4	314
D	R1EP-P	-
	R1P2-P	752
	R1P3-P	563
	R1P4-P	420

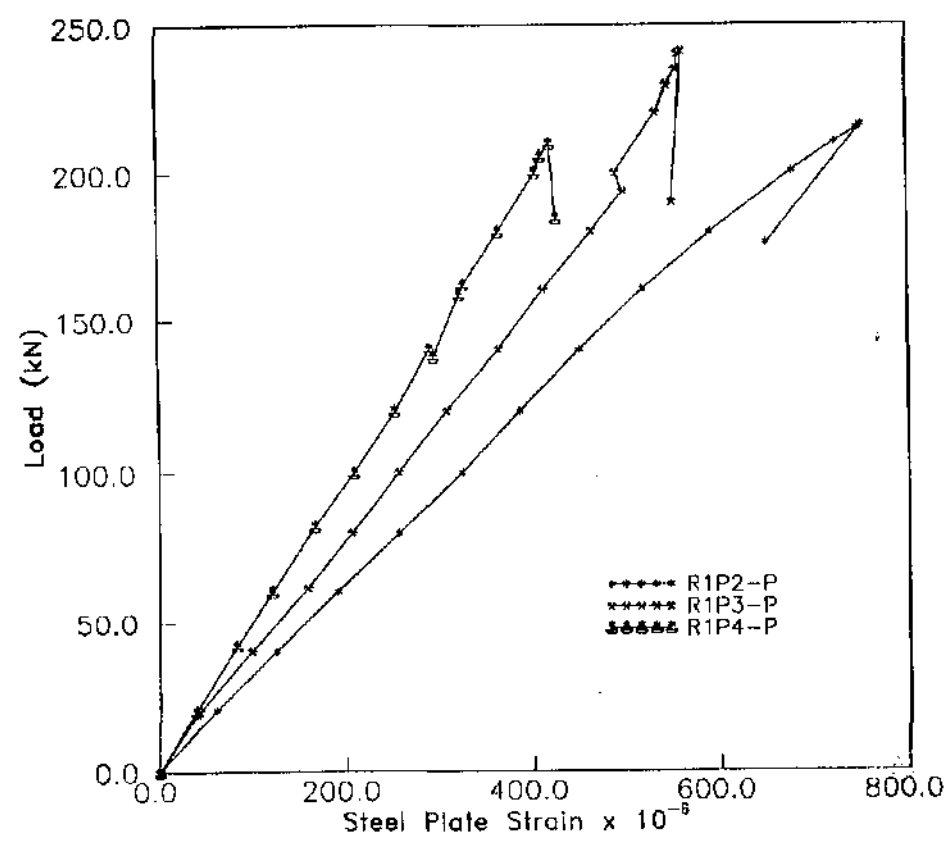


Fig. 4.11 Load versus Steel Plate Strain for Slabs in Series D

4.6.2 Composite Behaviour

Full composite action is one of the very important structural requirements in the plate bonding technique. To explore the effectiveness of epoxy glue in preserving the composite action between the plate, glue and concrete at all loading stages up to failure, slip was measured at two ends of the steel plate. The average results are shown in Table 4.10. The data show that composite action between the slab and external plate was preserved till failure.

The maximum slip recorded for the set of test slabs are generally very low (less than 1.00mm). Higher values like 1.930mm and 1.722mm were however recorded for slabs R0P4 and R1P4-P respectively. Zero or very low slip values indicate perfect bond and the composite slab behaves as a monolithic member with full interaction. On the other hand, higher slip values indicate bond failure which results in no interaction and the slab behaves individually. Although the slip measurements varied from 0.018mm to 1.930mm across the set of tested slabs, the effect of this became visible only on releasing the load after failure; when the plastically deformed plate often warped away from the concrete (see plate VII).

Examination of the plates revealed that the failure did not occur at the plate/epoxy or epoxy/concrete interfaces, but fracture invariably took place in the concrete cover.

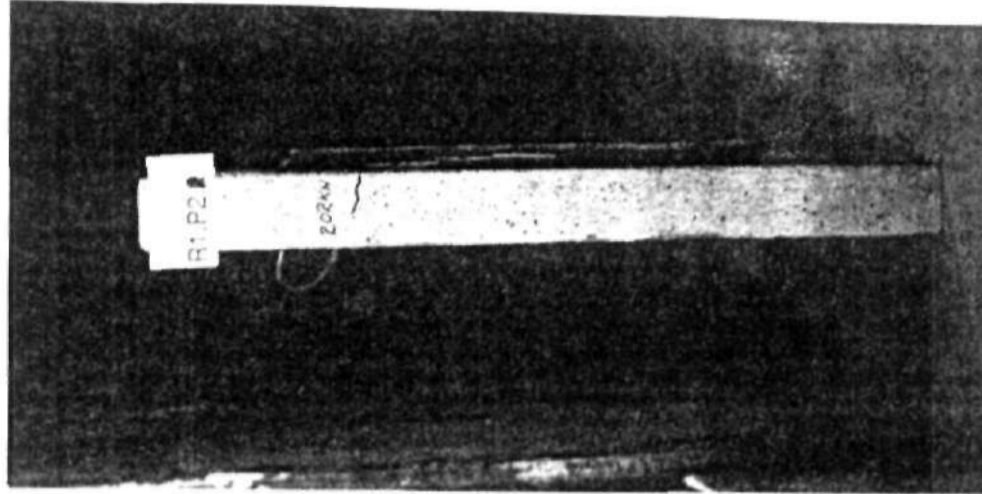


Plate VII Plate Separation and Fracture Effect.

Table 4.10 Observed Ultimate Slip of Test Slabs

Series No.	Slab No.	Ultimate Load (kN)	Ultimate Slip (mm)
A	R0P0	39	-
	R1P0	122	-
B	R1EP	173	-
	R1P2	224	0.018
	R1P3	237	0.706
	R1P4	240	0.495
C	R0P2	233	0.040
	R0P3	165	0.030
	R0P4	161	1.930
D	R1EP-P	153	-
	R1P2-P	216	0.822
	R1P3-P	241	0.028
	R1P4-P	210	1.722

4.6.3 Strength Properties

The effect of plating on the strength behaviour of the strengthened concrete slabs is important from a structural design point of view. The data presented in the previous sections show substantial reductions in deflection, steel plate strains and hence cracking at serviceability conditions. To evaluate this effect further, the loads carried by the plated slabs and those sustained by the unplated control slabs were compared.

The experimental first crack loads obtained by visual and auditory observations and ultimate loads are shown in Tables 4.11 and 4.12. The data indicate that the first crack load for slab R1P0 (in series A) was 41 percent higher than that of R0P0. For slab R1EP, the cracking load was about 2.11 times the value for slab R1P0. In terms of ultimate load capacity, slabs R1P0 and R1EP were respectively observed to be 3.13 and 4.54 times stronger than slab R0P0. Further, comparison of the ultimate capacity of R1P0 and R1EP revealed that the presence of the epoxy glue alone enabled the slab to carry higher loads by about 45 percent.

In the series (B), it was observed that the strengthened slabs have not only delayed the occurrence of the first crack but also controlled the widening and spreading of cracks to a significant extent. This is evidently seen

from Table 4.11 which indicates an increase of about 111 to 268 percent over the first crack load of the unplated reference slab R1P0. The ratio of the ultimate loads carried by plated slabs in this series to their first crack loads varied from 1.11 to 1.53. The ultimate carrying capacity of all strengthened slabs in the series were in excess of that of the control slab R1P0 and ranged from 45 to 98 percent. These results, therefore, indicate the beneficial effect of bonded plates on enhancing the ultimate flexural strength of conventional reinforced concrete slabs.

Table 4.11 Comparison of Strength Characteristics of Unplated Slab R1P0 and Plated Slabs in Series (B) and (D)

Series No.	Slab No.	1st Crack Load (kN)	Ult. Load (kN)	% over R1P0		Mean Ratio of Ult. Load Plated to Unplated
				1st Crack Load	Ult. Load	
B	R1EP	116	177	110.91	45.08	1.92
	R1P2	202	224	267.87	83.61	
	R1P3	186	237	238.18	94.26	
	R1P4	182	240	336.36	96.72	
D	R1EP-P	126	153	129.09	25.41	1.82
	R1P2-P	200	216	263.64	77.05	
	R1P3-P	194	241	252.73	97.54	
	R1P4-P	158	210	187.27	72.13	

Slabs R0P2 and R0P3 in series (C) showed an increase of about 287 percent in first crack loads over that of control slab R0P0 and for slab R0P4, its value was 295

percent more than the control slab R0P0 (Table 4.12). Although visually obtained data are subjected to errors, these results indicate the restraining effect of the epoxy-glued plate on the first cracking. The failure loads for all slabs in this series are also shown in Table 4.11. The ratio of the failure load to first crack load varied from a minimum of 1.10 to a maximum of 1.54 for all the slabs tested in this series. This corresponds to an increase in the flexural carrying capacity from 313 to 497 percent over that of reference slab R0P0.

The loads at which first cracking occurred in slabs of series (D) are also illustrated in Table 4.11. The results show high increases for strengthened slabs. The values ranged from about 129 to 264 percent over that of unplated slab R1P0. It was also observed that the first crack load appeared at about 75 to 93 percent of the measured ultimate load and the cracking plate strain varies from 322 to 678 micro-strains, as would be expected in structural members. The measured ultimate loads carried by all slabs in this series show that slabs precracked prior to plating were able to carry higher loads from 72 to 98 percent of the control slab R1P0.

It is also interesting to note that even precracked slab strengthened by epoxy glue only (i.e. R1EP-P) was effective in restoring the strength beyond that of the original slab R1P0. A comparison of their ultimate loads revealed that slab R1EP-P was stronger than slab R1P0 by about 25 percent.

Table 4.12 Comparison of Strength Characteristics of Slabs in Series (A) and (C) and Unplated Control Slab R0P0

Series No.	Slab No.	1st Crack Load (KN)	Ult. Load (KN)	% Over R0P0		Mean Ratio of Ult. Load Plated to Unplated
				1st Crack Load	Ult. Load	
A	R0P0	39	39	-	-	-
	R1P0	55	122	41.03	212.82	
C	R0P2	151	233	287.17	497.44	4.78
	R0P3	151	165	287.17	323.08	
	R0P4	154	161	294.87	312.82	

4.6.4 Cracking and Failure Characteristics

The overall cracking pattern of the test slabs across the series can be divided into four categories: pure flexural failure, pure shear failure, punching shear failure and

flexure-punching failure. Table 4.13 summarises the mode of failure of each slab; and typical crack patterns and failure modes are shown in plate VIII.

Table 4.13 Observed Modes of Failure

Series No.	Slab No.	Mode of Failure
A	R0P0	Rupture of Concrete
	R1P0	Punching Shear after Yielding Bars
B	R1EP	Punching Shear after Yielding of both Bars and Glue
	R1P2	Flexure-Punching followed by Plate Debonding
	R1P3	Flexure-Punching of Concrete after Yielding of Bars
	R1P4	Flexure-Punching of Concrete after Yielding of Bars
C	R0P2	Plate Yield and Concrete crushing by Shear
	R0P3	Plate Yield and Concrete Crushing by Shear
	R0P4	Plate Yield and Concrete Crushing by Shear
D	R1EP-P	Punching Shear after Yielding of both Bars and Glue
	R1P2-P	Flexure-Punching of Concrete after Yielding of Bars
	R1P3-P	Flexure-Punching of Concrete after Yielding of Bars
	R1P4-P	Flexure-Punching of Concrete after Yielding of Bars

Slab R0P0, because it had neither reinforcing bars nor steel plate, behaved in a highly brittle manner. It failed by rupture of concrete accompanied by a large

flexural crack at the centre. Pure shear failure occurred in slabs R0P2, R0P3 and R0P4 with concrete crushing after the yielding of steel plate. Near failure loads, the plate strains showed considerable spread yielding at the critical sections. There was no sign of debonding of the glue and concrete or plate prior to failure, nor was there any sign of cracking in the glue.

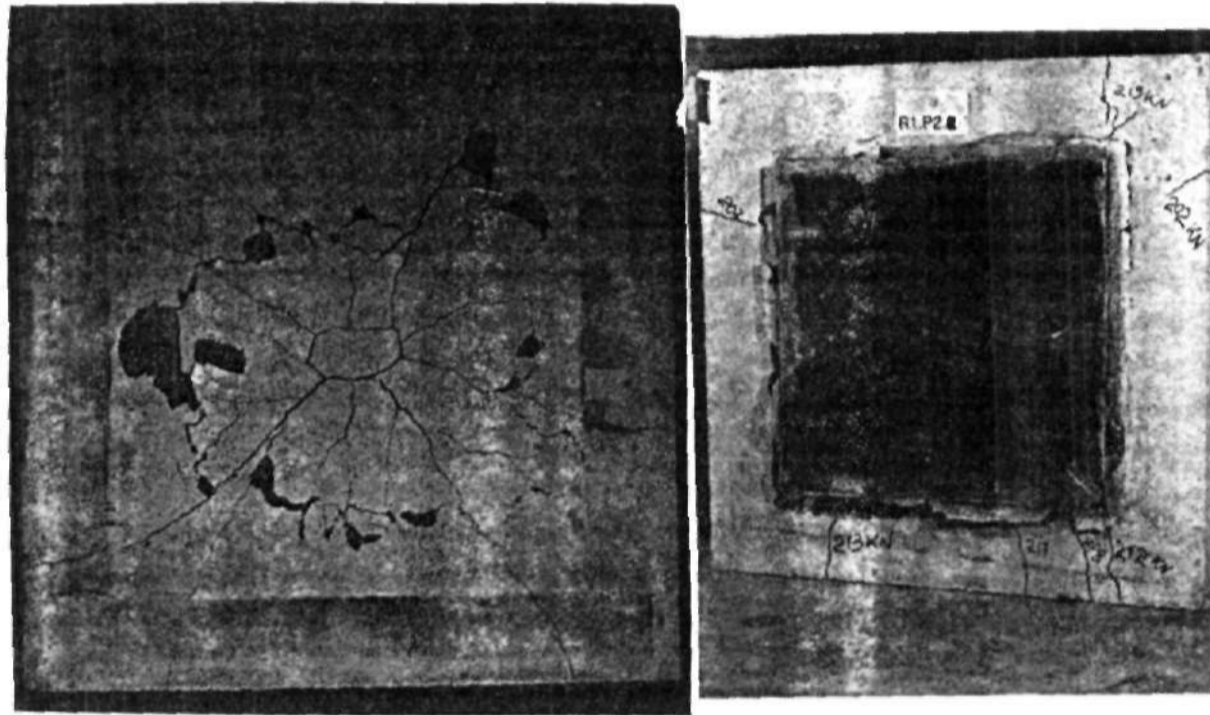


Plate VIII Cracking Behaviour and Failure Modes for Slabs Test Series (A) through (D)

For slabs failing in punching shear, R1P0, R1EP and R1EP-P, the crack patterns observed prior to punching consisted of side and tangential cracks, roughly at the loaded area, followed by radial cracking spreading from the loaded area. Final failure of these slabs took place by the load cell punching through the slab. Punching shear directly at the point of load appeared as a circle of diameter approximately equal to that of load cell. The punching cracks for these slabs occurred at about 90 to 95 percent of the maximum load. When punching occurred, the load fell suddenly to a value of approximately 20 percent of the ultimate load and was released completely in some cases.

For slabs failing by flexure-punching, all the plated slabs of series (B) and (D), punching failure occurred before the flexure yield lines were well developed. They were first formed at the sides then followed by radial cracking extending from the glue line. These cracks were much more pronounced along the lines parallel to the plate edges. As the load increased, tangential cracks under the edge of the load cell started appearing. Final failure developed by flexure-punching of concrete after yielding of reinforcing bars. Plate debonding (i.e. interface separation) was also observed in slab R1P2.

463595

However, apart from slab RiP2, none of the slabs in this category showed any sign of plate debonding from the glue and/or concrete at failure, but the concrete cover to the internal bars ripped away at the interface level. This was invariably initiated by flexural cracks at the end of the plate which propagated parallel to the glue line and eventually caused partial separation of the plate in some of these slabs. The punching shear crack for all slabs with this type of failure appeared between 80 to 95 percent of the maximum load and failure was generally sudden at the ultimate load.

CHAPTER 5

SUMMARY, CONCLUSIONS AND RECOMMENDATIONS5.1 Summary

The main purpose of this research work was to study the structural behaviour of epoxy plate bonded reinforced concrete slabs at the various limits of cracking, deflection and collapse. One of the objectives in the present study was the development of simple analytical models that predicted the ultimate response of concrete slabs strengthened with epoxy-bonded steel plates in the elastic and plastic stages. The analytical models were used to develop a simple algorithm which can be implemented on microcomputers.

The constitutive relationships used in the present algorithm are an elasto-plastic model for concrete and a bilinear model for reinforcing bars, steel plates and the bond element representing the interface between the plate and slab. An iterative procedure based on the principles of equilibrium of forces and compatibility of deformations was incorporated in the algorithm. The general approach was to assure a condition at the interface bond between the slab and steel plate; and check equilibrium while incorporating compatibility relationships. If equilibrium is not achieved, the force/deformation at the interface is adjusted until the internal forces are in equilibrium.

The algorithm was implemented in a computer program called PSLAB which was developed in FORTRAN 77.

Thirteen concrete slabs were tested to failure under central point bending. The measured load versus deflection at midspan of the slabs and the load versus strain in steel plate were plotted and compared with the control slabs. The results indicated that the addition of glued steel plates to reinforced concrete slabs can substantially increase their flexural stiffness, reduce cracking and structural deformations at all load levels, and contribute to a modest increase in their ultimate flexural capacity by up to about 98 percent. It was also observed that provided suitable epoxy glue with sufficient strengths and stiffness to transfer the shear force between the plate and concrete and adequate surface preparation are observed, plate bonding technique can effectively utilised to ensure composite behaviour and strengthened the slabs.

Comparisons of the test data obtained for thirteen concrete slabs with the analytical results showed a reasonably close agreement. The measured ultimate loads of almost all the slabs are within 16 percent of the calculated value.

5.2 Conclusions

The following conclusions can be drawn from the limited experimental results and analytical models for predicting structural behaviour and ultimate strength of plate bonded concrete slabs:

- (1) Strengthening of concrete slabs with epoxy-bonded steel plates enhances the ultimate flexural strength and stiffness of these members by controlling both cracking and deflection. This is due to the fact that the addition of plates in the tension face not only increases the area of tension steel, but also lowers the neutral axis, thereby reducing stresses in the existing reinforcement due to the applied load. The restraining effect of the epoxy glue and plate can be observed even on first cracking, and when the glue alone was present. The reduction in cracking and deformations increased with increasing plate thickness.
- (2) Variation in measured failure loads, as well as measured moment capacities are almost marginal and the plated reinforced concrete slabs are capable of carrying higher ultimate loads than the control unplated slabs, ranging from 1.82 times to 4.78 times.

- (3) Provided appropriate epoxy systems with a wide range of strengths and ductilities are selected and adequate precautions are observed plate bonding technique can be effectively utilised to ensure composite behaviour and strengthened the concrete slab.
- (4) The composite behaviour between the slabs and the external plate, is preserved till failure even though the maximum slip occurred at the ends of the plate is about 0.018 to 1.930 mm.
- (5) The method of epoxy bonding of steel plates can be advantageously adopted for improving the strength and stiffness of structurally damaged reinforced concrete slabs.
- (6) The addition of glued steel plates to precracked concrete slabs, which had been loaded to about 45 percent of their ultimate strength and plated under unloaded conditions, had no adverse effect on the flexural behaviour of the strengthened slabs. The restraining effect of the plates on existing cracks was, however, more pronounced when the load was increased beyond the original preloading value. The precracked slabs were able to carry higher ultimate load from 72 to 98 percent. The presence of glued alone also enable the slabs to carry higher loads by as much as 45 percent.

- (7) The general assumptions used in the development of the analytical models were such that the models were easily formulated and implemented in simple microcomputer programme. Although simplified, the models are very suitable in predicting the strength of strengthened slabs in which flexure controls the behaviour. However, it should not be used if slabs are suspected to fail from diagonal tension. Since no shear provisions were accounted in the models. It should be noted that reinforced concrete slabs are designed to fail in flexure and not in shear. Therefore, this limitation is not a practical constraint.
- (8) The comparison of the test data and analytical results based on the equilibrium of forces and compatibility of deformations showed that the behaviour of strengthened slabs can be predicted with reasonable accuracy. However, due to the actual extensive deformations and the model's linear strain assumptions, the calculated values are in average lower than the real ones.
- (9) The ratio of the experimental and the calculated load capacities varies from 0.64 to 1.20. However, the calculated values of almost all the slabs are within 16 percent from the measured ultimate load values.

This fact demonstrates the accuracy of PSLAB in predicting flexural strength of reinforced concrete slabs. Also, the calculated deflection values in almost all the slabs are lower than the measured ones. This indicates that an excessive spread of plasticity along the slabs, leads in most cases in larger than possible to predict deflections.

- (10) Flexural-Punching cracking dominated the failure of slabs in series B and D while shear-flexure cracks characterised the failure of slabs in series A and C.
- (11) There is a limit to plate thickness that would be structurally desirable for a conventional reinforced concrete slab. For the tests in this study, slabs with 3mm thick plates appeared to meet the design criteria for plated beams as recommended by Swamy et al (1987).

5.3 Recommendations

Before this novel strengthening technique can be applied in practice, the following further studies are recommended to address additional issues:

- (1) Studies must be undertaken to establish criteria for predicting the limiting load that causes the concrete layer between the reinforcing bars and steel plates to fail.

- (2) Effect of environmental factors, like temperature and moisture on the bond at the interface of concrete and steel plate, as well as the performance of strengthened slabs under sustained loading and fatigue should be examined.
- (3) Studies on different types of epoxies and steel plates to select optimum combination should also be conducted.
- (4) The percentage of reinforcing bars in slabs and its effect on the selection of the area of steel plates should be investigated.
- (5) Strains in the reinforcing bars and the resulting effect on crack propagation is also another area to be examined.

REFERENCES

1. American Concrete Institute Committee 503, (1992). Guide for the Selection of Polymer Adhesives with Concrete. The American Concrete Institute Material Journal, 89(1): pp. 90-105.
2. American Concrete Institute Committee 503, (1984). Use of Epoxy Compounds with Concrete. ACI 503R-80, Detroit, Michigan.
3. American Concrete Institute Committee 318, (1984). Building Code Requirements for Reinforced Concrete. ACI 318-84, Detroit Michigan.
4. American Concrete Institute, (1968). Epoxies with Concrete. ACI Special Publication No. 21, Detroit, Michigan.
5. Anandarajah, A. and Vardy, A. E. (1985). A Theoretical Investigation of the Failure of Open Sandwich Beams due to Interfacial Shear Fracture. The Structural Engineer, 63B(4): pp. 85-92.
6. Araldit for a Bridge Bonded Reinforcing Instead of Replacement, (1979). Ciba-Geigy, Aspekto, Switzerland, 4, pp. 2-4.
7. ASTM, 1973. Annual Book of ASTM Standards, Part 4, American Society for Testing and Materials, 1973. (Standards for Deformed steel bars A588). Philadelphia, Pennsylvania, USA.
8. BS 4461:1969. Cold Worked Bars for the Reinforcement of Concrete. British Standards Institution, London, 1969.
9. BS 1449:1970. Steel Plate, Sheet and Strip: Part 1. Carbon Steel flat Products. British Standards Institution, London, 1970.
10. Birkeland, P. W. and Birkeland, H. W. (1966). Connection in Precast Concrete Construction. The American Concrete Institute Journal, 63(3): pp. 345-367.
11. Chung, H. W. (1981). Epoxy Repair of Bond in Reinforced Concrete Member. The American Concrete Institute Journal, 78(1).
12. Chung, H. W. and Lui, L. M. (1978). Epoxy Repaired Concrete Joints Under Dynamic Loads. The American Concrete Institute Journal, 75(7): pp. 313-316.

13. Chung, H. W. (1977). Epoxy Repaired Concrete Joints. The American Concrete Institute Journal, 74(6).
14. Chung, H. W. (1975). Epoxy Repaired Reinforced Concrete Beams. The American Concrete Institute Journal, 72(5).
15. Cook, J. P. (1967). The Bonded Aggregate Composite Beam. Final Report to Deck-Guard Corporation, Albany, New York.
16. CP110:1972. The Structural Use of Concrete: Parts 1, Code of Practice for Design, Materials and Workmanship. British Standards Institution, London, 1972.
17. Davies, B. L. and Powell, J. (1984). Strengthening of Brisworth Road Bridge, Rotherham. In IABSE 12th Congress, Vancouver, BC, pp. 401-407.
18. Dussek, I. J. (1980). Strengthening of Bridge Beams and Similar Structures by Means of Epoxy-Resin-Bonded External Reinforcement. Transportation Research Record 785, Transportation Research Board, pp.21-24.
19. Fleming, G. J. and King, G. E. M. (1967). The Development of Structural Adhesives for Three Original Uses In South Africa. In Proceedings of RILEM International Symposium on Synthetic Resins in Building Construction, Paris, pp. 75-92.
20. Hamoush, S. A. and Ahmad, S. H. (1990). Debonding of Steel Plate Strengthened Concrete Beams. The Journal of Structural Engineering ASCE 116(2): pp. 356-371.
21. Hognestad, E., Hanson, N. W. and McHenry, D. (1955). Concrete Stress Distribution in Ultimate Strength Design. In Proceedings of American Concrete Institute Journal, 52(4): pp. 455-480.
22. Hugenschmidt, H. (1975). Epoxy Adhesive for Concrete and Steel. In Proceedings of 1st International Congress on Polymers in Concrete, London, The Construction Press Ltd, Hornby, 1976, pp 195-209.
23. Irwin, C. A. K. (1975). The Strengthening of Concrete Beams By Bonded Steel Plates. TRRL Supplementary Report 160 UC, Transport and Road Research Laboratory, Department of the Environment, Crowthorne, UK, p8.
24. Johnson, R. P. and Tait, C. J. (1981). The strength in Combined Bending and Tension of Concrete Beams with Externally Bonded Reinforcing Plates. Building and Environment, 16(4): pp.287-299.

25. Jones, R., Swamy, R. N. and Charif, A. (1988). Plate Separation and Anchorage of Reinforced Concrete Beams Strengthened by Epoxy-Bonded Steel Plates. The Structural Engineer, 66(5/1): pp. 85-94.
26. Jones, R., Swamy, R. N., Bloxham, J. and Bouderbalah, A. (1980) Composite Behaviour of Concrete Beams with Epoxy Bonded External Reinforcement. The International Journal of Cement Composites, 2(2): pp. 91-107.
27. Kar, J. N. and Sharma, Y. (1992). Tests on Epoxy Bonded Concrete and Reinforced Concrete Elements. The Indian Concrete Journal, pp. 327-331.
28. Kajfasz, S. (1967). Concrete Beams with External Reinforcement Bonded by Gluing. In proceedings of RILEM International Symposium on Synthetic Resins in Building Construction, Part 2, Paris, pp. 142-151.
29. Klaiber, F. W., Dunker, K. F., Wipf, T. J. and Sanders, W. W. Jnr, (1987). Methods of Strengthening Existing Highway Bridges. Transportation Research Board Report No. 293, National Cooperative Highway Research Programme (NCHRP).
30. Ladner, M. and Webber, C. (1985). Concrete Structures with Bonded External Reinforcement. EMPA Report No. 705, Dübendorf.
31. Ladner, M. (1983). Reinforced Concrete Members with Subsequently Bonded Steel Sheets. In proceedings of IABSE Symposium on Strengthening of Building structures - Diagnosis and Therapy, Venezia, Final report, 46: pp. 203-210.
32. Lerchenthal, H. (1967). Bonded Sheet Metal Reinforcement for Concrete Slabs. In RILEM International Symposium on Resins in Building Construction, Paris, pp. 165-173.
33. L'hermite, R. L. and Bresson, J. (1967). Concrete Reinforced with Glued Plates. In Proceedings of RILEM International Symposium on Synthetic Resins on Building Construction, Paris, pp. 175-203.
34. Lino, T. and Otokawa, K. (1981). Application of Epoxy Resins in Strengthening of Concrete Structures. In proceedings of 3rd International Congress on Polymers in Concrete, Koriyama, Japan, pp. 997-1011.
35. Lloyd, G. D. and Calder, A. J. J. (1982). The Microstructure of Epoxy Bonded Steel-to-Concrete Joints. Supplemental Report No. 705, Transport and Road Research Laboratory, Structures Department, Bridge Division, Crowthorne, Berkshire, England.

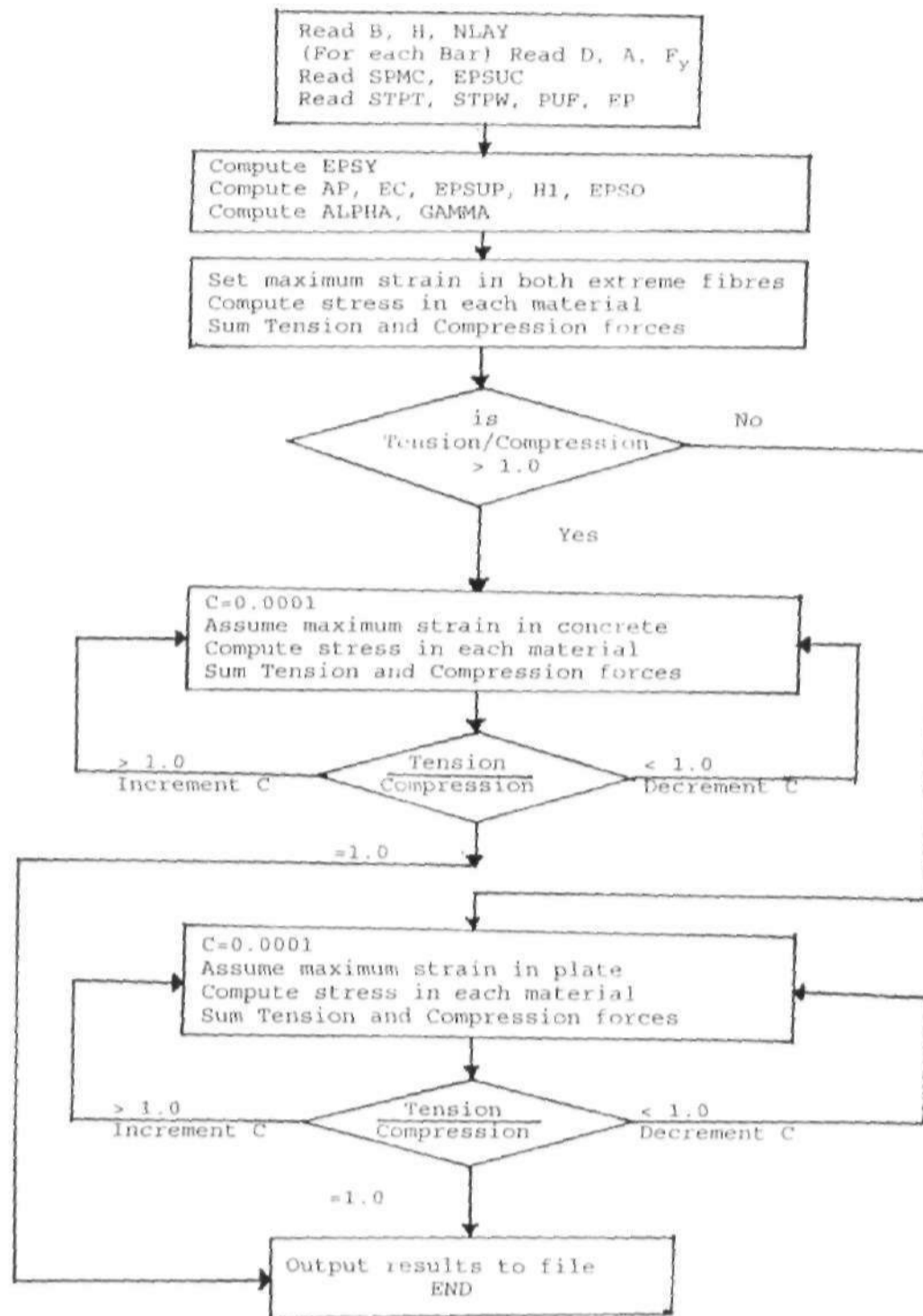
36. MacDonald, M. D. (1978). The Flexural Behaviour of Concrete Beams with Bonded External Reinforcement. TRRL, Supplementary Report No. 415, Transport and Road Research Laboratory, Department of Environment, Crowthorne, UK, p13.
37. Maeda, Y., Matsui, S., Shimada, I. and Kato, H. (1980). Deterioration and Repairing of Reinforced Concrete Slabs of Highway Bridges in Japan. Technology Reports (Osaka University), 30(1599): pp. 135-144.
38. Mander, R. F. (1974). Bonded External Reinforcement, a Method of Strengthening Structures. Department of the Environment Report on Quinton Interchange for the M5 Motorway.
39. Mays, G. C. and Hutchinson, A. R. (1989). Engineering Property Requirements for Structural Adhesives. In proceedings of Institution of Civil Engineers, Part 2, 85: pp. 485-501.
40. Moss, P. J. (1984). Structural Uses of Epoxy Resin Adhesives. Road Research Unit, Bulletin 68, ISSN 0549-0030, National Road Board, University of Canterbury, Wellington, New Zealand.
41. Nawy, E. G. (1984). Shear Transfer in 2-Layer Composite Systems. National Transportation Board, Washington, DC.
42. Oehlers, D. J. and Moran, J. P. (1990). Premature Failure of Externally Plated Reinforced Concrete Beams. The Journal of Structural Engineering, ASCE, 116(4): pp.978-995.
43. Oehlers, D. J. (1992). Reinforced Concrete Beams with Plates Glued to Their Soffits. The journal of Structural Engineering, ASCE, 118(8): pp. 2023-2038.
44. Ong, K. C. G. and Cusens, A. R. (1982). Flexural Tests of Steel-Concrete Open Sandwiches. The Magazine of Concrete Research, 34(102): pp. 130-138.
45. Park, R. and Paulay, T. (1975). Reinforced Concrete Structures. John Wiley and Sons, Inc., New York, 769pp.
46. Parkinson, J. (1978). Glue Solves a Sticky Problem for Gestetner. New Civil Engineering, 310: pp. 26-27.
47. Plecnik, J. M., Fogarty, J. H. and Kurfees, J. R. (1986). Behaviour of Epoxy Repaired Beams Under Fire. The Journal of Structural Engineering, ASCE, 112(4): pp.906-922.

48. Raithby, K. D. (1980). External Strengthening of Concrete Bridges with Bonded Steel Plates. TRRL Supplementary Report 612, Transport and Road Research Laboratory, Department of the Environment, Crowthorne, Berkshire, England.
49. Raju, N. K. and Nadgir, N. S. (1991). Limit State Behaviour of Reinforced Concrete Beams Strengthened by Epoxy-Bonded Steel Plates. The Indian Concrete Journal, pp. 124-129.
50. Rao, M. V. B., Ali, M. S. M., Kurmi, D. P. and Kumar, N. (1992). Strengthening of Reinforced Concrete Beams by External Plates attached with Expanding Bolts. The Indian Concrete Journal, pp. 509-513.
51. Roberts, T. M. (1989). Approximate Analysis of Shear and Normal Stress Concentrations in the Adhesive Layer of Plated Reinforced Concrete Beams. The Structural Engineer, 67(12/20): pp.229-233.
52. Roberts, T. M. and Haji-Kazimi, H. (1989). A Theoretical Study of the Behaviour of Reinforced Concrete Beams Strengthened by Externally Bonded Steel Plates. In the Proceedings of the Institution of Civil Engineers, Part 2, 87: pp. 39-55.
53. Roberts, T. M. (1988). Plate Separation and Anchorage of Reinforced Concrete Beams Strengthened by Epoxy-Bonded Steel Plates. (Correspondence). The Structural Engineer, 67(12/21): pp.187-188.
54. Saadatmanesh, H., Albrecht, P. and Ayyub, B. M. (1989a). Experimental Study of Prestressed Composite Beams. The Journal of Structural Engineering, ASCE, 115(9), pp. 2349-2364.
55. Saadatmanesh, H., Albrecht, P. and Ayyub, B. M. (1989b). Analytical Study of Prestressed Composite Beams. The Journal of Structural Engineering, ASCE, 115(9), pp. 2365-2382.
56. Saadatmanesh, H., Albrecht, P. and Ayyub, B. M. (1989c). Guidelines for Flexural Design of Prestressed Composite Beams. The Journal of Structural Engineering, ASCE, 115(11), pp. 2944-2961.
57. Saadatmanesh, H. and Ehsani, M. R. (1990). Fibre Composite Plates Can Strengthen Beams. The Concrete International, pp. 65-71.
58. Saemman, J. C. and Washa, G. W. (1964). Horizontal Shear Connections Between Precast Beams and Cast-In-Place Slabs. In Proceedings of American Concrete Institute, 61(11): pp. 1383-1409.

59. Sinno, R. and Furr, H. Bonded Concrete Overlays. The Journal of Structural Engineering, ASCE, 96, pp. 1627-1638.
60. Solomon, S. K. and Gopalani, L. K. (1979). Flexural Tests on Concrete Beams Externally Reinforced by Steel Sheet. The Indian Concrete Journal, pp. 249-253.
61. Solomon, S. K., Smith, M. D. and Cusens, A. (1976). Flexural Tests of Steel-Concrete-Steel Sandwiches. The Magazine of Concrete Research, 28(94): pp. 13-20.
62. Swamy, R. N., Jones, R. and Charif, A. (1989). The Effect of External Plate Reinforcement on the Strengthening of Structurally Damaged Reinforced Concrete Beams. The Structural Engineer, 67(3/7): pp.45-56.
63. Swamy, R. N., Jones, R. and Bloxham, J. W. (1987). Structural Behaviour of Reinforced Concrete Beams Strengthened by Epoxy-Bonded Steel Plates. The Structural Engineer, 65A(2): pp.59-68.
64. Triantafillou, T. C. and Plevris, N. (1992). Strengthening of Reinforced Concrete Beams with Epoxy-Bonded Fibre Composite Materials. Materials and Structures, 25, pp. 201-211.
65. Van-Gemert, D. A. and VandernBosch, M. C. J. (1985). Repair and Strengthening of Reinforced Concrete Structures by Means of Epoxy Bonded Steel Plates. International Conference on Deterioration, Bahrain, pp. 181-192.
66. Van-Gemert, D. A. (1981). Repairing of Concrete Structures by Externally Bonded Steel Plates. In Proceedings of ICP/RILEM/IBK, International Symposium on Plastics in Material and Structural Engineering, Prague, Czechoslovakia, 1982, Elsevier Scientific Publishing Company, 1982, pp. 519-526.
67. Viest, M. I. (1960). Review of Research on Composite Steel Concrete Beam. The Journal of Structural Engineering, ASCE, 86(ST6).
68. Yam, L. C. P. (1981). Design of Composite Steel-Concrete Structures. Surrey University Press, Glasgow.
69. Yam, L. C. P. and Chapman, J. C. (1972). The Inelastic Behaviour of Continuous Beams of Steel and Concrete. In Proceedings of Institution of Civil Engineers, 53, pp. 487-501.

LIST OF APPENDICES

APPENDIX I PSLAB FLOWCHART



APPENDIX II - PSLAB COMPUTER PROGRAM

```

C*****
C*
C*          **** PSLAB ****
C*
C*          THIS PROGRAMME ANALYSES A CONCRETE SLAB
C*          TO WHICH A STEEL PLATE MAY BE BONDED TO THE TENSION FACE
C*
C*          FORMAT OF INPUT FILE, "PSLAB.IN" :
C*          H          (DEPTH OF SLAB, MM.)
C*          B          (WIDTH OF SLAB, MM.)
C*          L          (SPAN LENGTH OF SLAB, MM.)
C*          NLAY      (NUMBER OF LAYERS OF REINFORCEMENTS)
C*          D(1)      (DEPTH OF CENTROID OF THE LAYER FROM THE TOP OF
C*                   THE SLAB, MM.)
C*          A(i)      (AREA OF REINFORCEMENTS AT THIS DEPTH, SQ MM.)
C*          Fy(i)     (TENSILE STRENGTH OF REINFORCEMENTS AT THIS
C*                   DEPTH, N/SQ MM.)
C*                   (REPEAT D,A,Fy FOR EACH LAYER)
C*          EPSY      (MAXIMUM STRAIN FOR THE REINFORCEMENTS IN EACH
C*                   LAYER, DIMENSIONLESS)
C*          SPMC      (CONCRETE STRENGTH, N/SQ MM.)
C*          EC        (CONCRETE MODULUS, N/SQ MM.)
C*          EPSO      (STRAIN AT WHICH PARK AND PAULAY MODEL CHANGES
C*                   FORMULAE, DIMENSIONLESS)
C*          EPSuc     (MAXIMUM CONCRETE STRAIN, DIMENSIONLESS)
C*          ALPHA     (RESULTANT FACTOR OF MAGNITUDE OF COMPRESSION)
C*          GAMMA     (RESULTANT FACTOR OF LOCATION OF COMPRESSION)
C*          STPt      (THICKNESS OF STEEL PLATE, MM.)
C*          STPw      (WIDTH OF STEEL PLATE, MM.)
C*          Fyp       (TENSILE STRENGTH OF STEEL PLATE, N/SQ MM.)
C*          Ep        (ELASTIC MODULUS OF STEEL PLATE, N/SQ MM.)
C*          Ap        (CROSS SECTIONAL AREA OF STEEL PLATE, SQ MM.)
C*          EPSup     (ULTIMATE STRAIN FOR STEEL PLATE, DIMENSIONLESS)
C*          H1        (DISTANCE FROM CENTRE OF STEEL PLATE TO TOP OF
C*                   CONCRETE)
C*
C*****

          DIMENSION D(10), A(10), Fy(10), EPSO(10), EPSY(10)
C *** OPEN FILES
C   OPEN (1, FILE='PSLAB.IN', STATUS='OLD')
C   OPEN (2, FILE='PSLAB.OUT', STATUS='NEW')
C   OPEN (3, FILE='DEBUG.OUT', STATUS='UNKNOWN')
C *** YOUNGS MODULUS FOR STEEL IS ASSUMED CONSTANT
          ES = 200000.0
          L = 900
C *** I/O
          WRITE(*,*)'GIVE VALS:B,H,NLAY'
          READ (*,*)B,H,NLAY
          DO 1, K=1, NLAY
          WRITE (*,*)'GIVE VALS:D(K),A(K),Fy(K)'
          READ (*,*) D(K), A(K), Fy(K)
C *** MAXIMUM STRAIN FOR THE REINFORCEMENTS IN EACH LAYER

```

```

        EPSY(K) = Fy(K) / ES
1      CONTINUE
        WRITE(*,*)'GIVE VALS:SPMC, EPSUC, STPT, STPW, FYP, EP'
        READ (*,*) SPMC, EPSUC, STPT, STPW, FYP, EP
        READ (1,*) STPT, STPW, Fyp, Ep
C *** IF NO PLATE IS APPLIED, ZERO ALL THE PLATE VARIABLES
        IF(STPT.EQ.0.0.OR.STPW.EQ.0.0.OR.Fyp.EQ.0.0.OR.EP.EQ.0.0) THEN
            STPT = 0
            STPW = 0
            Fyp = 0
            Ep = 0
            END IF
        WRITE (2,*) 'CONCRETE='
        WRITE (*,80)B,H,SPMC, EPSUC
        WRITE (2,80) B,H,SPMC, EPSUC
        WRITE (*,*) 'REINFORCEMENT='
        WRITE (2,*) 'REINFORCEMENT='
        WRITE (2,*) 'LAYER=', ' DEPTH=', ' AREA=', ' Fy='
        DO 2,K=1,NLAY
            WRITE (2,81) K,D(K),A(K),Fy(K)
2      CONTINUE
        WRITE (*,*) 'PLATE= '
        WRITE (2,*) 'PLATE='
        IF (STPT.EQ.0.0) THEN
            WRITE (*,*) 'NO PLATE SPECIFIED'
            WRITE (2,*) 'NO PLATE SPECIFIED'
        ELSE
            WRITE (*,*) 'THICKNESS=', 'WIDTH=', 'Fyp=', 'Ep='
            WRITE (2,82) STPT, STPW, Fyp, Ep
            WRITE (2,*) ' '
C *** CROSS SECTIONAL AREA OF PLATE
            Ap = STPT*STPW
C *** YOUNG'S MODULUS FOR CONCRETE
            EC = 5000 * (SPMC)**0.5
C *** ULTIMATE STRAIN FOR PLATE
            IF (STPT.EQ.0.0) THEN
                EPSUP=0
            ELSE
                EPSUP=Fyp/Ep
            END IF
C *** DISTANCE FROM CENTRE OF PLATE TO TOP OF CONCRETE
            H1=H+STPT/2.
C *** INITIALISE COMPRESSION, TENSION, MOMENTS AND LOCATION OF NEUTRAL
            AXIS
            CC=0.
            T=0.
            CM=0.
            C=.0001
C *** STRAIN AT WHICH PARK AND PAULAY EQUATION FOR STRESS CHANGES
            EPSO(K)=2.*SPMC/EC
C *** FIND ALPHA AND GAMMA
            IF(EPSUC.LT.EPSO(K)) THEN
                ALPHA=(EPSUC/EPSO(K))-(1./3.)*(EPSUC/EPSO(K))**2.
                GAMMA=1-(8*EPSO(K)-3*EPSUC)/(4*(3*EPSO(K)-EPSUC))
            ELSE
                AX=1000.*EPSO(K)-4

```

```

      ALPHA=(2*EPSO(K))/(3*EPSUC) +
      $(850*EPSO(K)+75*EPSUC-4)/AX -
      $(EPSO(K)/EPSUC)*(925*EPSO(K)-4)/AX
      BX = 175.*EPSO(K)**3.-EPSO(K)**2.-150.*EPSUC**3.
      $+6.*EPSUC**2.-1275.*EPSO(K)*EPSUC**2.
      CX = 12.*EPSUC-4.*EPSO(K)+775.*EPSO(K)**2. -
      $2550.*EPSUC*EPSO(K)-225.*EPSUC**2.
      GAMMA = 1-BX/(EPSUC*CX)
      END IF
C *** CALCULATE INTERNAL FORCES ASSUMING A BALANCED FAILURE CONDITION
      IF (STPT.EQ.0.0) THEN
      CB = EPSUC * D(NLAY) / (EPSUC + EPSY(NLAY))
      ELSE
      CB = EPSUC * H1 / (EPSUC + EPSUP)
      END IF
      CC = ALPHA*SPMC*B*CB
      CM = CC*(CB - GAMMA*CB)
      DO 7, K=1,NLAY
      EPSO(K) = EPSUC * ABS(CB - D(K)) / CB
      IF (EPSO(K).GT.EPSY(K)) EPSO(K) = EPSY(K)
      IF (D(K).LT.CB) THEN
      CC = CC + EPSO(K) * ES * A(K)
      ELSE
      T = T+EPSO(K) * ES * A(K)
      END IF
      CM = CM + ABS(EPSO(K) * ES * A(K) * (CB - D(K)))
7      CONTINUE
      T = T + Fyp * Ap
      CM = CM + Fyp * Ap * (H1-CB)
C *** ETA SHOWS HOW CLOSE TO A BALANCED CONDITION A
C *** PARTICULAR APPLICATION OF PLATE IS.
      ETA = T/CC
      WRITE (2,90) ETA
C *** BRANCH TO CALCULATE MOMENTS FOR EITHER CASE
      IF (ETA.LT.1.0) THEN
      IF (STPT.EQ.0.0) THEN
      WRITE (2,100)'TENSION REINFORCEMENT YIELDING'
      ELSE
      WRITE (2,100)'PLATE FRACTURE'
      END IF
10     CONTINUE
      CC = 0.
      CM = 0.
      T = 0.
      CC = ALPHA * SPMC * B * C
      CM = CC * (C - GAMMA*C)
      DO 25, K=1,NLAY
      IF (STPT.EQ.0.0) THEN
      EPSO(K) = EPSY(NLAY) * ABS(C - D(K)) / (D(NLAY) - C)
      ELSE
      EPSO(K) = EPSUC * ABS(C - D(K)) / (H1 - C)
      END IF
      IF (EPSO(K).GT.EPSY(K)) EPSO(K) = EPSY(K)
      IF (D(K).LT.C) THEN
      CC = CC + EPSO(K) * ES * A(K)
      ELSE

```

```

      T = T + EPSO(K) * ES * A(K)
      END IF
      CM = CM + ABS(EPSO(K) * ES * A(K) * (C-D(K)))
25  CONTINUE
      IF (STPT.NE.0.0) THEN
        EPSP = EPSUP
        T = T + EPSP * Ep * Ap
      END IF
      CM = CM + EPSP * Ep * Ap * (H1-C)
      ETA = T/CC
      IF (ABS(1.0-ETA).LT.0.001) THEN
        WRITE (2,110) CM
      ELSE IF (ETA.GT.1.0) THEN
        C = C + 0.1
        GOTO 10
      ELSE
        C = C - 0.001
        GOTO 10
      END IF
      ELSE IF (ETA.GT.1.0) THEN
        WRITE (2,100) 'CONCRETE CRUSHING'
30  CONTINUE
        CC = 0
        CM = 0
        T = 0
        CC = ALPHA * SPMC * B * C
        CM = CC * (C - GAMMA*C)
        DO 45, K=1,NLAY
          EPSO(K) = EPSUC * ABS(C - D(K)) / C
          IF (EPSO(K).GT.EPSY(K)) EPSO(K) = EPSY(K)
          IF (D(K).LT.C) THEN
            CC = CC + EPSO(K) * ES * A(K)
          ELSE
            T = T + EPSO(K) * ES * A(K)
          END IF
          CM = CM + ABS(EPSO(K) * ES * A(K) * (C - D(K)))
45  CONTINUE
          IF (STPT.NE.0.0) THEN
            EPSP = EPSUC * (H1-C) / C
            IF (EPSP.GT.EPSUP) EPSP = EPSUP
            T = T + EPSP * Ep * Ap
          END IF
          CM = CM + EPSP * Ep * Ap * (H1-C)
          ETA = T/CC
          IF (ABS(1.0-ETA).LT.0.001) THEN
            WRITE (2,110) CM
          ELSE IF (ETA.GT.1.0) THEN
            C = C + 0.1
            GOTO 30
          ELSE
            C = C - 0.001
            GOTO 30
          END IF
          ELSE
            WRITE (2,100) 'BALANCED FAILURE CONDITION'
            WRITE (2,110) CM

```

```
      END IF
      END IF
C *** CALCULATE CURVATURE, DEFLECTION, AND LOAD
      CURV = EPSUC / C
      DEFL = (L**2) * CURV / 12
      P = 2.0 * CM / L
      WRITE(2,70)CM,CURV,DEFL,EPSP,EPSUC,P
80     FORMAT (1X,F6.1,9X,F6.1,9X,F5.1,11X,F6.4)
81     FORMAT (1X,I3,11X,F5.2,10X,F7.1,9X,F5.1)
82     FORMAT (1X,F5.3,9X,F6.1,1X,F5.1,7X,F8.1)
90     FORMAT ('T/CC BAL:',F8.1)
100    FORMAT ('MODE OF FAILURE: ',A)
110    FORMAT ('BENDING MOMENT: ',F11.1,' N-MM.')
```

300 FORMAT (F10.6,3X,F10.6,3X,F10.6,3X,F10.6)

70 FORMAT (1X,F11.1,2(1X,F9.5),1X,F7.5,1X,F8.6,1X,F10.2)

```
      STOP
      END
```

APPENDIX III - TYPICAL DESIGN CALCULATIONS FOR TEST SLABDESIGN LOADAssumed Data:

Slab dimensions: 1100 x 1100 x 100 mm with a clear span of 900 mm

Characteristics strength of materials:

Concrete, $f_c = 35 \text{ N/mm}^2$

Steel, $f_y = 400 \text{ N/mm}^2$

Bar size = 10 mm

Concrete cover, $c = 20$ (Assuming mild exposure)

Basic span - effective depth ratio = 20

Density of reinforced concrete = 24 kN/m^3

Live load = 7.5 kN/m^2

LOAD ESTIMATION

$$\text{Self weight of slab} = 100 \times 24 \times 10^{-3} = 2.4 \text{ kN/m}^2$$

$$\text{Plaster, floor finishes and others, allow} = 1.6 \text{ kN/m}^2$$

$$\text{Total characteristic dead load, } g_k = 4.0 \text{ kN/m}^2$$

$$\text{Total characteristic live load, } q_k = 7.5 \text{ kN/m}^2$$

$$\text{Service load, } n_s = 1.0g_k + 1.0q_k \text{ ---- [cl.2.3.4.1(CP110)]}$$

$$= (4.0 + 7.5)$$

$$= 11.5 \text{ kN/m}^2$$

For a 1 m width of slab

$$\text{Ultimate load, } n_u = 1.4g_k + 1.6q_k \text{ ---- [cl.2.3.3.1(CP110)]}$$

$$= [(1.4 \times 4.0) + (1.6 \times 7.5)] \times 1$$

$$= 17.6 \text{ kN/m}$$

CHECKING FOR TWO-WAY ACTION

$l_y/l_x = 0.9/0.9 = 1.0$ =====The slab is spanning in two directions
 Since the slab spans in two directions, the maximum moments are given by

$$M_{sx} = a_{sx} n_u l_x^2 \quad \text{in direction of span } l_x$$

and

$$M_{sy} = a_{sy} n_u l_x^2 \quad \text{in direction of span } l_y$$

where M_{sx} and M_{sy} are the moments at mid-span on unit strips of unit width with spans l_x and l_y respectively, and n_u is as defined above. a_{sx} and a_{sy} are moment coefficients from Table 12(CP110).

For a square slab like this one, $a_{sx} = a_{sy} = 0.062$

$$\begin{aligned} \text{Effective depth, } d &= h - c - \phi/2 = 100 - 20 - 10/2 \\ &= 75 \text{ mm} \end{aligned}$$

The area of reinforcement (per metre width) in directions l_{sx} and l_{sy} respectively are

$$A_{sx} = \frac{M_{sx}}{0.87 f_y z}$$

and

$$A_{sy} = \frac{M_{sy}}{0.87 f_y z}$$

where f_y is the characteristic strength of steel and z the lever arm is given by

$$z = l_d = d$$

$$l_d = \text{lever arm factor from chart D1(CP110)}$$

The effective depth d used in calculating A_{sy} is taken to be less than that for A_{sx} because of the different depths of the two layers of reinforcement.

BENDING IN l_y Span

$$\begin{aligned} M_{sx} &= a_{sx} n_u l_x^2 = 0.062 \times 17.6 \times 0.92 \\ &= 0.8839 \text{ kNm} \end{aligned}$$

$$\frac{M_{sx}}{bd^2 f_c} = \frac{0.8839 \times 10^6}{1000 \times 75^2 \times 35} = 0.0052$$

$$\eta_s = 0.95 \quad (\text{Chart D1CP110})$$

$$\begin{aligned} z &= 75 \times 0.95 \\ &= 71.25 \text{ mm} \end{aligned}$$

$$A_s = \frac{M_{sx}}{0.87 x f_y z} = \frac{0.8839 \times 10^6}{0.87 \times 400 \times 71.25} = 35.65$$

$$A_s = 35.65 \text{ mm}^2 / \text{m}$$

Minimum area of reinforcement for mild steel is given by

$$\begin{aligned} A_{smin} &= 0.25 \% \text{ bd} \quad (\text{cl.3.11.4.1 CP110}) \\ &= 0.0025 \times 1000 \times 75 \\ &= 187.50 \text{ mm}^2 / \text{m} \end{aligned}$$

Since the minimum reinforcement is greater than the calculated,

A_{smin} is provided in form of

R4 at 59 mm centres ($A_s = 239 \text{ mm}^2 / \text{m}$)

Span - Effective Depth Ratio

$$\frac{100A_s}{bd} = \frac{100 \times 239}{1000 \times 75} = 0.32$$

From table 10CP110, for service stress $f_s = 235 \text{ N/mm}^2$ the span - effective depth modification factor = 1.3

$$\text{limiting} \frac{\text{span}}{\text{effective depth}} = 20 \times 1.3 = 26$$

$$\text{actual} \frac{\text{span}}{\text{effective depth}} = \frac{900}{75} = 12$$

Thus $d = 75 \text{ mm}$ is adequate.

BENDING IN l_y SPAN

$$\begin{aligned} M_{sy} &= \alpha_{sy} n_u l x^2 = 0.062 \times 17.6 \times 0.9^2 \\ &= 0.8839 \text{ kNm} \end{aligned}$$

Since the reinforcement for this span will have a reduced effective depth, take

$$z = 71.25 - 4 = 67.25 \text{ mm}$$

$$A_s = \frac{M_{sy}}{0.87 f_y z} = \frac{0.8839 \times 10^6}{0.87 \times 400 \times 67.25} = 32.77$$

$$A_s = 32.77 \text{ mm}^2 / \text{m}$$

Also provide $A_{s\text{min}} = 187.50 \text{ mm}^2 / \text{m}$ in the form

R4 at 59 mm centres ($A_s = 239 \text{ mm}^2 / \text{m}$)

$$\frac{100 A_s}{bh} = \frac{100 \times 239}{1000 \times 100} = 0.24$$

which is greater than 0.15, the minimum transverse steel.

SHEAR

$$\text{Shear force, } V = \frac{n_s x l}{2} = \frac{17.6 \times 0.9}{2} = 7.92 \text{ kN}$$

$$\text{Shear stress, } v = \frac{V}{bd} = \frac{7.92 \times 10^3}{1000 \times 75} = 0.11$$

From Table 5CP110, ultimate shear stress, $v_c = 0.43 \text{ N/mm}^2$ and from Table 14CP110, modification factor, $\xi_s = 1.30$ and $\xi_s v_c = 1.30 \times 0.43 = 0.56 \text{ N/mm}^2$.

Therefore, since $v < \xi_s v_c$ no shear reinforcement is required.

LOCAL BOND

For 4 mm bars at 59 mm centres,

$$\text{Perimeter } \sum U_s = \frac{1000 \times 3.14 \times 4}{59} = 213 \text{ mm per metre width}$$

$$\text{Local bond stress, } f_{bs} = \frac{V}{\sum U_s d} = \frac{7.92 \times 10^3}{213 \times 75} = 0.5 \text{ N/mm}^2$$

From Table 21CP110, ultimate local bond stress = $3.0 \text{ N/mm}^2 > 0.5 \text{ N/mm}^2$

END ANCHORAGE

$$f_{bs} = 0.50 < 3.0/2$$

Therefore, anchorage length $\geq 30 \text{ mm}$ or (End bearing)/3

But End bearing = 230 mm

Therefore, Anchorage length = $230/3 = 77 \text{ mm}$, beyond centre line of the support.